Journal of Geology & Geophysics
ISSN: 2381-8719

Kanouo et al., J Geol Geophys 2017, 6:4
DOI: 10.4172/2381-8719.1000298

Research Article Open Access

Petro-geochemistry, Genesis and Economic Aspects of Mafic Volcanic Rocks in the West and Southern Part of The Mamfe Basin (SW Cameroon, Central Africa)

Nguo Sylvestre Kanouo[1]*, Rose Fouateu Yongue[2], Tanwi Richard Ghogomu[2,3], Emmanuel Njonfang[4], Syprien Bovari Yomeun[2] and Emmanuel Archelaus Afanga Basua[5]

[1]Mineral Exploration and Ore Genesis Unit, Department of Mines and Quarries, Faculty of Mines and Petroleum Industries, University of Maroua, Cameroon'
[2]Department of Earth Sciences, University of Yaoundé I, Cameroon
[3]Department of security, Quality and Environment, Faculty of Mines and Petroleum Industries, University of Maroua, Cameroon'
[4]Higher Teachers Training School, University of Yaoundé I, Cameroon
[5]Department of Earth Sciences, China University of Geosciences wuhan, China

Abstract

Geologic prospecting, petrographic and geochemical analyses of mafic volcanic exposures in the west and southern part of the Mamfe Basin (SW Cameroon) distinguishes: basanites, picro-basalts, alkali basalts and tholeiitic basalts. They are relatively LREE-enriched, undersaturated, saturated or oversaturated due to presence or absence of normative nepheline, hypersthene or quartz. Basanites mainly form pillow-like lavas, and are aphyric or porphyritic. They have significant concentration of Ni (up to 387 ppm) and Ba (up to 436 ppm). These alkaline rocks cooled from less evolved mantle source magma. Picro-basaltic fragments exclusively found in the western part of the basin are Ni (up to 259 ppm) Ba (up to 2090 ppm) -enriched porphyritic, alkaline or subalkaline rocks. They also cooled from less evolved mantle source magma. Basalts form volcanoclasts, flow and dykes. They are aphyric or porphyritic, alkaline, transitional or subalkaline. Some of these rocks are Al-enriched. They crystallized from variably evolved mantle source magma within the Oceanic Island Basalt and Continental Rift Basalt tectonic settings.

Keywords: Cameroon; Mamfe basin; Mafic volcanic rock; Geologic prospecting; Petrography; Geochemistry; Alkaline; Tholeiitic

Introduction

Mafic volcanic rocks are melanocratic to mesocratic igneous rock which crystallized from a basaltic magma within the oceanic and continental crust [1-4]. Rocks from basaltic magma are varied with different petrographic, physical and geochemical features whose determination lead to their characterization and to a better understanding of their condition of formation [1,2,5-7]. They occur as aa, pillow, columnar or pahoehoe lava flow, or form dyke and sill which are easy to recognize in the field [2,7-9]. Some of these rocks are mineralized (e.g., host interesting PGE concentration: or can host gemstones as xenocrysts and in xenoliths sourced from other rocks by the ascending magma) [10-13]. Sulfide metallic mineralizations are associated with pillow basalts in the Yaeyama Central Graben, Southern Okinawa Trough, Japan [14]. Native iron is found in some basaltic rocks in Buhl basalts (Kassel Germany) and Siberian flood basalts [15-17]. FeO-Al_2O_3-TiO_2 rich rocks are found associated with transitional tholeiitic lava flows in the Tertiary Bana plutono-volcanic complex in the continental sector of the Cameroon Volcanic Line [18]. Peridotite xenoliths with significant Ni-Co concentrations are hosted in basaltic lavas in Kumba (SW region of Cameroon) [19]. Basaltic rocks can be mined as industrial mineral used for building and road construction [20,21]. Thus, mafic rocks have both scientific and economic interests.

The Mamfe Sedimentary Basin in the SW region of Cameroon (Figure 1) encloses mainly uncharacterized mafic flows, fragments, and dykes found in both the sedimentary part of the basin and some rocks of the basement [22]. These mafic rocks crop out in the west, south and south-east of the Manyu Division, which hosts the basin. Most of these rocks are recorded as basaltic with no specific identification. Although some of those rocks were petrographically characterized, information is limited for most of them. Wilson and Dumort presented a field reconnaissance report and constructed a map, respectively [23,24]. Kanouo presented field data and major element geochemical feature for mafic volcanic flow and volcano clasts found in the western part of the basin [22]. Much still has to be done to identify and characterize these rocks and verify if they have any interests in mining industries. Gem corundum and coarse zircon are found in detrital sediments (in Nsanaragati) at about 10 km east of the nearest basaltic flow (in Ekok) [22,25]. Although not yet confirmed, the presence of diamond within sedimentary clasts in the western part of Mamfe Basin is mentioned in Laplaine and Soba [26]. Studies carried out on corundum and zircon show that they are largely from magmatic crystallizations with some zircon being from kimberlitic origin [22,27-30]. Research studies carried out in South-East Asia, Australia and in many gem corundum fields in the world have shown that, alkali basalts can host corundum as xenocrysts or in xenoliths [31,32]. The origin of corundum found in the western part of the Mamfe Basin is still debated. During this research study a series geological prospecting was carried out in many volcanic terrains and localities found in the Mamfe Basin in order to locate gem or metallic host rocks.

In this paper, we present field data, petrographic and geochemical results for mafic volcanic rocks found in the west and southern part of the Mamfe Basin in order to characterize those rocks, understand the history of their genesis and present their economic aspects.

***Corresponding author:** Nguo Sylvestre Kanouo, Department of Mines and Quarries, University of Maroua, Cameroon; Tel: +237678966240, +237678966240; E-mail: skdasse@gmail.com, sylvestrekanouo@yahoo.fr

Received June 01, 2017; **Accepted** July 18, 2017; **Published** July 25, 2017

Citation: Kanouo NS, Yongue RF, Ghogomu TR, Njonfang E, Yomeun SB, et al. (2017) Petro-geochemistry, Genesis and Economic Aspects of Mafic Volcanic Rocks in the West and Southern Part of The Mamfe Basin (SW Cameroon, Central Africa). J Geol Geophys 6: 298. doi: 10.4172/2381-8719.1000298

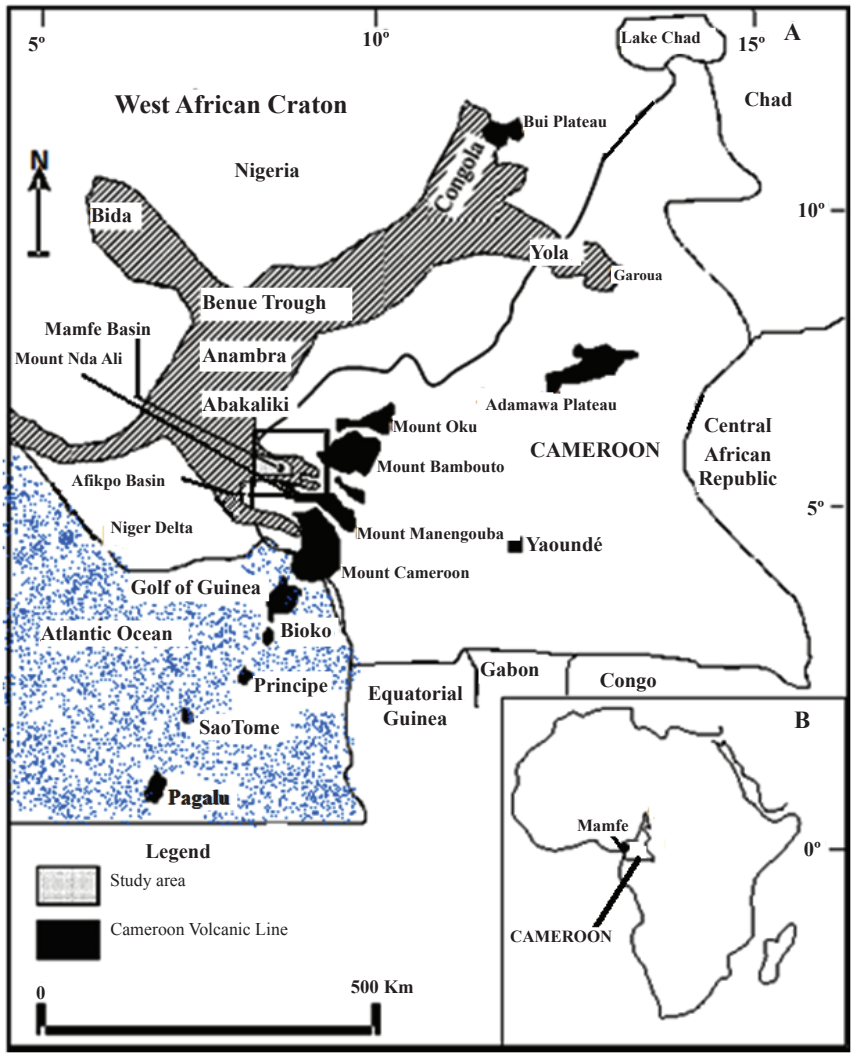

Figure 1: (A) and (B) location of the Mamfe sedimentary basin in the regional context [76,77].

Geography and geologic setting

The Mamfe Sedimentary Basin located between 5°30' to 6°00'N and 8°15' to 9°45' E underlies a coastal plain in Cameroon with low to slightly high relief whose heights range from 30 to 300 m [22,24]. It is locally bordered by high igneous terrains (e.g., Mount Nda Ali: 1200 m, Mount Mbinda: 1000 m, Nkogho hills: up to 600 m). The basin is regionally bordered by upland areas (Figure 1) (e.g., Mount Rumpi, Bambouto, Bamenda, Manengouba and Koupé), which are part of the Cameroon Volcanic Line [33,34]. The Mamfe Basin is administratively situated in the Manyu Division made up of four sub-divisions (Mamfe Center, Eyumojock, Upper Bayang, and Akwaya) and occupied by three main ethnic groups: the Kenyangs, Akwayas, and Ejagham [22]. The climate in this Division is hot and humid and consists of a rainy and a dry season modified by the deviation of the monsoon and the relief of Mount Cameroon [35]. The vegetation is dominantly that of the equatorial rain forest [22]. The drainage system is principally that of the Cross River (Figure 2) whose main source is found in Mount Bambouto [36]. The sources of its main tributaries the Munaya and Badi Rivers are at the Mount Rumpi and Nda Ali respectively [22].

The Mamfe Basin is an assigned Cretaceous age intracontinal sedimentary filled depression whose opening is related to the Atlantic Ocean and is one of the south eastern branches of the Benue Trough in Nigeria [24]. It is suggested to be genetically related to that of the Benue Trough as they both have similar structures [24,37]. The Mamfe Sedimentary Basin is filled by very fine to very coarse-grained immature and mature siliciclastic lithified sediments (e.g., conglomerates, sandstones, arkoses, shales and mudstones) [22,37-42]. These are locally associated with evaporites [23,24,43-45]. Part of these rocks (e.g., shales in Bachuo Ntia and Etoko) are good potential hydrocarbon sources [42]. Sedimentary rocks in the west of the Mamfe Basin are locally overlain by recent detritus enclosing gemstones of magmatic and metamorphic origin [22,28,30]. Lithified sediments in this basin are also locally overlain or cross-cut by basaltic, phonolitic, or trachytic rocks probably formed from post sedimentary volcanism [22,23,46,47]. These exposures are underlain by assumed Precambrian age basement made up of granites, gneisses, migmatites, syenites, and mica-schists (Figure 2) and undated gabbros, diorites, syenites, and monzonites at the Mount Nda Ali [22-24,46,48]. Part of the Precambrian rocks encloses polycrystalline, recrystallized and fractured quartz, and kinked biotite probably arising from post-crystallization cataclastic deformation [22].

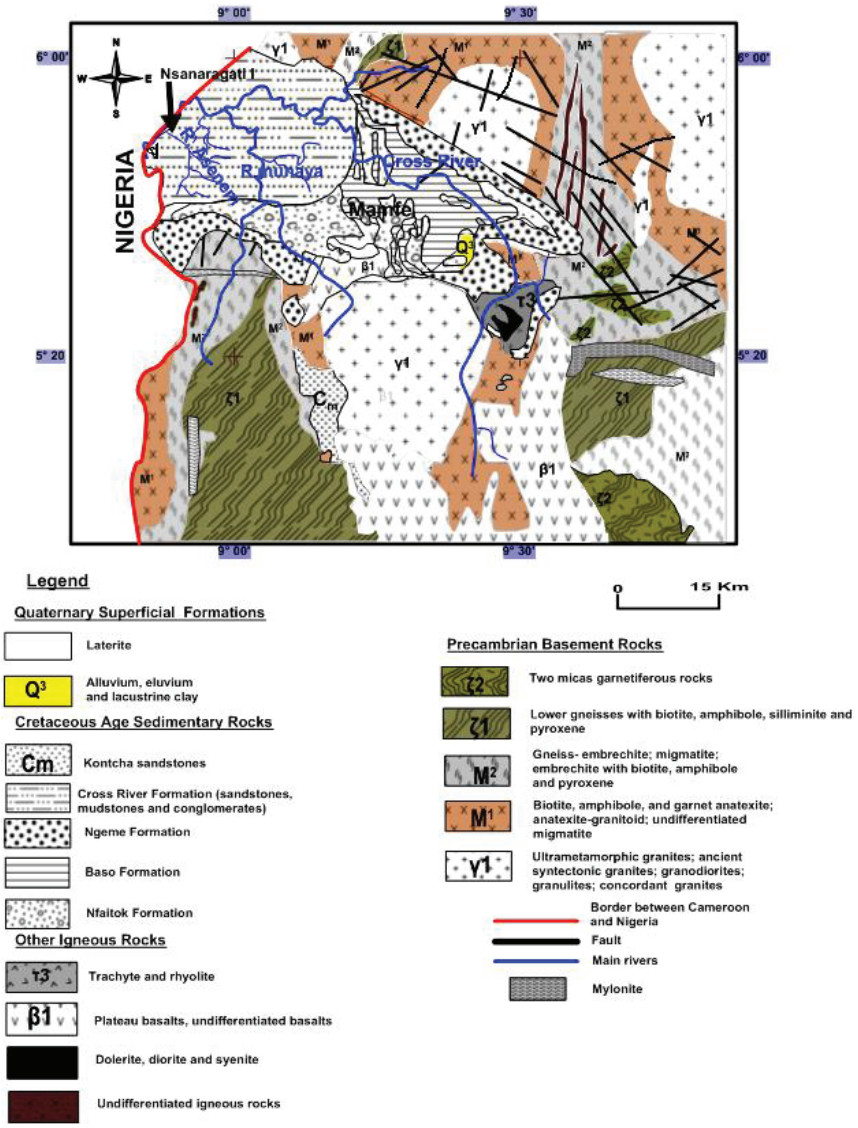

Figure 2: Sketch geological map showing Asenem River flowing on sedimentary formations in the western part of the Mamfe Basin; modified from Dumort [24] and Eyong [39].

Field work and analytical methods

With the aim to prospect, locate and characterize the mafic rocks and any associated gemstone sources and metallic mineralization, detailed geologic surveys were carried out in western and southern Mamfe basin. A total of ten villages (Ekok, Nsanaragati, Otu, Araru, Nkogho, Mbiofong, Babi, Ogurang, Ossing, and Kembong) were surveyed, outcrops were described and more than one hundred rock fragments were collected from flows, dykes, alluviums, colluviums and eluviums. The sampled rocks were macroscopically and microscopically characterized, and their geochemical features determined. The description of the outcrops included: outcropping mode; colour, size, and shape (for fragments); width, length, strike and dip (for a dyke or sill); nature of the surface, width, and height (for flows); presence of any xenoliths and/or xenocrysts; type and nature of host and underlying rock; and the relationship between the mafic rock and surrounding geologic formations. The macroscopic description of collected fragments was based on criteria presented in and Winter [1,2,7].

More than fifty thin sections were prepared at the Geology and Mining Research Institute (Yaoundé-Cameroon) and later characterized under the petrographic microscope (EUROMEX) at the Department of Earth Sciences of the University of Yaoundé I. Particular attention was paid to the presence of xenocryst during the macroscopic characterization. The characterization was based on parameters such as texture, colour of minerals, shape, weathering and mineral replacement, relief, extinction angle, interference colour as defined in Mackenzie et al., Mackenzie and Adams, Mackenzie and Guilford, Higgins and Beaux et al. [3,49-52].

Twenty samples were analyzed to determine their elementary abundance in China and South Africa. The major and minor elemental concentration in seven samples (NKK3, NKK4, NKK5, NKK7, KEG, TAE, OSG) was determined by an X-ray fluorescence spectrometer in China. The analytical procedures used to acquire these results are similar to those presented in Wu et al. [53]. Thirteen selected samples (e.g., NSI1, BAI3, BAI4, ARK16) were analyzed for their major, minor,

trace and rare earth elements contents at ALS Chemex South Africa (Pty) Ltd, Johannesburg Gauten. These results were obtained by ICP-AES (Inductively Coupled Plasma-Atomic Emission spectroscopy) and ICP-MS (Inductively Coupled Plasma-Mass Spectroscopy). Major, minor (with Loss on Ignition) and selected trace element contents (e.g., Pb, Mo, Cd, As, Cu, Zn, Sc, and Ag) were determined by ICP-AES. A prepared sample (0.200 g) was added to lithium metaborate/lithium tetraborate flux (0.90 g), mixed well and fused in a furnace at 1000°C. The resulting melt was then cooled and dissolved in 100 ml of 4% nitric acid/2% hydrochloric acid. This solution was then analyzed by ICP-AES and the results were corrected for spectral inter-element interferences. Oxide concentration was calculated from the determined elemental concentration and the result was reported in that format. If required, the total oxide content was determined from the ICP analyte concentrations and loss on Ignition (L.O.I.) values. A prepared sample (1.0 g) was placed in an oven at 1000°C for one hour, cooled and then weighed. The percent loss on ignition was calculated from the difference in weight. Base metals can be reported with the ME-MS81 by a four acid digestion but not all elements were quantitatively extracted. A prepared sample (0.25 g) is digested with perchloric, nitric, hydrofluoric and hydrochloric acids. The residue was topped up with dilute hydrochloric acid and the resulting solution was analyzed by ICP-AES. Results were corrected for spectral inter-element interferences. Most of the trace elements (e.g., Ba, Cr, Ga, Hf, Ta, Th, U, V, Sn, Rb, Sr, Zr, and Y) and all the REE were quantified by ICP-MS. A prepared sample (0.200 g) was added to lithium borate flux (0.90 g), mixed well and fused in a furnace at 1000°C. The resulting melt was then cooled and dissolved in 100 ml of 4% HNO_3/ 2% HCl solution. This solution is then analyzed by inductively coupled plasma mass spectrometry. Results for Co and Mo were not obtained by this method.

Results

The mafic rocks are first classified using the analytical results. The named rocks are then described on field nature, macroscopic and microscopic petrography and major and trace element (including REE) results.

Nomenclature and field description

Nomenclature: The major element data as oxides (Table 1), were plotted on the total alkali versus silica diagram with a subalkaline-alkaline dividing line, for each rock's classification (Figure 3) [54]. A few plots lie in the sub-alkaline field and on the dividing line, while most have alkaline affinity. The major element compositions plotted on Le Bas et al. binary total alkali versus silica diagram (Figure 3) shows that the samples range from basanite to picro-basalt, and basalt [5].

Field description: Basanites crop out at the center of Ekok, Babi, and Nkogho. They form dark grey and massive lava flows with some being much more vesicular than others. At Ekok, two generation of flows include a vesicle-enriched flow underlying a less vesicular flow (Figure 4a and 4b). The contact between the flows is partly made up of well cemented pebble to cobble size sedimentary clasts (Figure 4b). The vesicle-enriched flow locally overlies a less consolidated conglomerate. The upper flow has a less developed top soil. In Nkogho, outcropping pillow lava partly overlies granitic bedrock. The surface of each flow is uneven and full of regular and irregular cracks similar to those of vesicle-enriched basanite at Ekok. Basanite at Babi occurs as scattered fragments within soils around some hills. Picro-basalts outcrops south west of Ekok and show variable shape with smooth blocky fragments overlying fine to coarse-grained sandstones (Figure 4c). Fragments are scattered in reddish clastic soil found on the only hill (up to 200 m high). Basalts form dykes, fragments (in alluvium, colluvium and/or eluvium) and/or flows in Nkogho, Babi, Araru, Nkogho, Kembong, Talangaye, Ossing, and Nsanaragati. A NE-SW trending vertical dyke more than 30 m length and up to 50 cm width cross-cuts granitic basement SE of Nkogho (Figure 4d). It is dark grey and massive with vesicles locally filled with white matter and is separated by a very thin dark layer, a probable product of a contact metamorphism. Just west and north, other basalts include volcanoclasts (colluviums and eluviums) associated with granitic fragments and sandstones in streams, while to the North West these clasts overlie granitic pegmatite and sandstone. Volcanoclasts also appear NW of Asenem River (in Nsanaragati). Variable shaped basalt fragments are widespread in Nkogho and Ossing, and locally found in Talangaye and Babi, while basaltic lava flow localities found in Ossing, Talangaye, Kembong, and Araru. They form a patch on granitic basement in Kembong, and overlie mica-schist in Araru, but contacts between the lava and surrounding rocks were not visible in Ossing and Talangaye.

Petrography: In Ekok, vesicles are less 10% in vesicle-depleted basanites (Figure 5a) and more than 30% in vesicle-enriched basanites

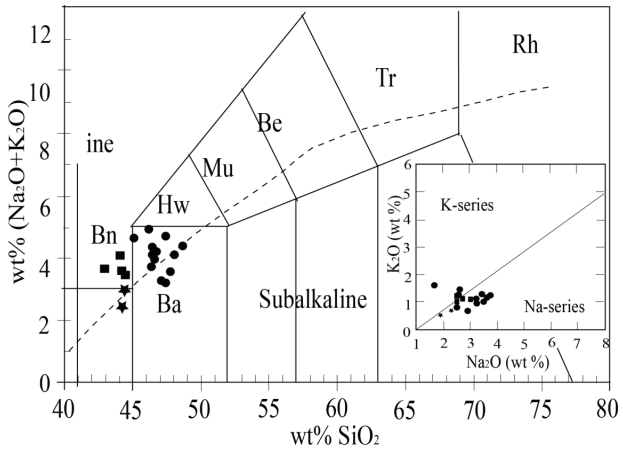

Figure 3: Total alkali *vs.* silica (T.A.S.) classification diagram for the west and southern Mamfe volcanic rocks [5]. Inset: Na_2O *vs.* K_2O subdivision diagram of the alkaline series [59]. The alkaline-subalkaline dividing line is from Irvine and Baragar [54]. The square (basanites), star (picro-basalts) and rounded spots (basalts).

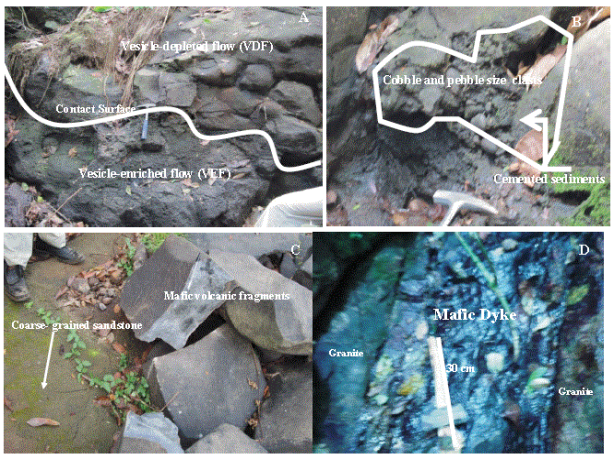

Figure 4: Mafic volcanic rocks outcrops in the west and southern part of the Mamfe Basin (a and b: basanites in Ekok; c: picro-basalt in Ekok; d: basaltic dyke in Nkogho).

Sample composition	Basanites				Picro-basalts		Basalts													
(wt.%)	NKK3	BAI3	EKK1	EKK3	EKK6	EKK11	NSI2	NSI3	NKK1	NKK2	NKK4	NKK5	NKK6	NKK7	NKK10	ARK16	KEG2	TAE2	OSG	BAI4
Si2O	42.95	44.1	44.4	44.2	44.4	44.2	46.4	46.3	46.4	46.7	46.14	46.36	48	47.4	48.6	47.4	47.05	45.06	46.58	47.7
Ti2O	3.55	2.54	2.27	2.31	2.28	2.27	2.32	2.32	2.74	2.65	3.27	3.15	2.49	3.2	2.74	0.8	2.73	3.08	2.94	3.54
Al203	12.4	12.4	13.05	13	13.5	13.3	13.45	13.3	13.85	13.7	13.48	13.56	13.6	13.97	14.7	15.35	15.35	13.81	13.32	14.05
Fe2O3*	13.97	12.55	12.6	12.4	11.85	12.05	12.15	11.95	12.8	12.7	13.75	13.32	12.9	12.98	10.75	12	12.43	13.32	13.57	13.5
MnO	0.19	0.18	0.2	0.18	0.18	0.16	0.19	0.18	0.16	0.16	0.17	0.17	0.16	0.19	0.17	0.22	0.16	0.18	0.25	0.17
MgO	10.78	13.15	11.4	11.35	10.2	11.3	9.58	10	8.97	8.5	8.05	8.2	8.45	7.07	7.06	8.2	5.79	8.38	7.63	5.49
CaO	9.06	8.64	9.98	9.87	10.05	9.64	9.45	9.28	9.22	9.29	9.31	9.24	9.08	9.32	9.91	10.5	9.19	9.51	9.54	9.07
Na2O	2.48	3	2.47	2.53	2.29	1.87	3.17	2.54	2.98	3.14	3.72	2.93	3.19	3.55	3.44	1.66	2.49	3.39	2.59	2.89
K2O	1.18	1.08	1	1.06	0.7	0.54	1.2	1.22	1.1	1.09	1.2	1.19	0.94	1.16	0.98	1.55	0.78	1.27	1.4	0.67
P2O5	0.69	0.69	0.57	0.6	0.59	0.52	0.55	0.55	0.56	0.55	0.52	0.55	0.48	0.58	0.5	0.08	0.51	0.74	0.62	0.45
Cr2O3	-	0.09	0.05	0.06	0.05	0.05	0.06	0.06	0.03	0.03	-	-	0.04	-	0.04	0.04	-	-	-	0.01
LOI	2.62	1.36	1.56	1.96	2.87	3.5	0.93	2.63	1.33	1.48	0.48	1.13	1.11	0.47	1.25	2.02	3.07	1.1	1.31	2.02
Total	99.87	99.79	99.56	99.53	98.99	99.42	99.47	100.35	100.15	100	100.09	99.8	100.46	99.89	100.16	99.82	99.55	99.84	99.75	99.56
Al2O3/TiO2	3.49	4.88	5.74	5.63	5.92	5.86	5.78	5.73	5.05	5.17	4.12	4.3	5.46	4.37	5..36	19.19	5.62	4.48	4.53	3.97
Na2O/ K2O	2.1	2.77	2.27	2.39	3.27	3.46	2.64	2.08	2.71	2.88	3.1	2.46	3.39	3.06	3.51	1.07	3.19	2.67	1.85	4.31
(Na2O+ K2O)-(0.37*SiO2-14.43)	2.2	2.19	1.47	1.67	0.99	0.49	1.63	1.06	1.34	2.78	2.28	1.4	0.8	1.6	0.87	0.1	0.29	2.42	1.19	0.34
Mg#	56.51	63.82	60.37	60.65	59.17	61.23	56.7	58.5	54.13	52.98	49.64	50.9	52.45	47.84	52.51	53.5	43.96	51.07	48.63	40.64
CIPW normative Wt (%)																				
Quartz																	12.73	2	8.22	3.13
Orthoclase	6.38		5.78	5.83	5.74	3.83	2.97	6.52	6.67	0.97	5.86	6.39	6.36	5.12	6.23	5.31	8.41	4.78	7.6	8.4	3.61
Albite	18.55		16.33	20.61	16.36	17.95	14.74	23.22	19.9	23.17	24.17	22.87	22.41	24.87	27.29	26.69	12.9	21.84	29.05	22.26	22.29
Anorthite	17.59		15.56	21.27	19.23	22.69	24.49	17.39	19.7	19.45	18.25	14.89	18.38	18.44	17.04	19.97	27.41	29.44	18.95	20.91	21.32
Nepheline	0.36		3.61		1.76			0.77		-	-	2.96	-	-	-	-	-	-	-	-	-
Diopside	15.39		15.27	17.92	17.59	15.98	13.13	17.7	15.47	15.2	16.32	18.8	15.83	15.89	17.1	17.71	16.15	4.02	14.97	11.84	13.71
Wollastonite	-		-	-	-	-	-	-	-	-	-	-	-	-	-	-	-	1.91	-	1.24	-
Hypersthene	-		-	6.81	-	4.24	13.16	-	8.02	4.52	1.69	-	4.4	10.25	1.17	3.5	10.04	-	0.21	-	11.01
Olivine	15.54		21.15	4	17.55	14.11	9.95	12.14	7.93	8.66	11.23	9.47	8.62	2.82	7.34	6.7	7.54	-	-	-	-
Magnetite	18.54		16.48	18.02	16.47	15.92	16.27	17.05	17.05	17.05	16.75	17.95	17.45	17.23	17.09	14.29	15.98	18.68	19.56	19.99	17.84
Ilmenite	6.17		4.37	4.25	4.02	4.01	4.02	4.05	4.08	4.78	4.58	5.59	5.41	4.36	5.52	4.77	1.4	5.37	5.92	5.67	6.13
Apatite	1.46		1.45	1.3	1.27	1.27	1.27	1.17	1.18	1.19	1.16	1.08	1.15	1.02	1.22	1.06	0.17	1.22	1.74	1.46	0.95

Table 1: Major element abundance (in wt. %) and CIPW norm in mafic volcanic rocks from the west and southern part of Mamfe Basin (Manyu Division, SW Cameroon). [Mg#=100 × (MgO/40.31)/(MgO/40.31)+Fe_2O_3 × 0.8998/71.85 × (1-0.15), assuming Fe_2O_3/ Fe_2O_3+FeO)=0.15. Recalculated to 100% anhydrous; total iron is expressed as Fe_2O_3; LOI: Loss 0n Ignition. Sample Location, EKK: Ekok; BAI: Babi; NSI: Nsanaragati; NKK: Nkogho; ARK: Araru; KEG: Kembong; TAE: Talangaye; and OSG: Ossing].

Figure 5: Hand specimens for mafic volcanic rocks from the west and southern part of the Mamfe Basin (a and b: basanites; c and d: picro-basalts; e and f: basalts).

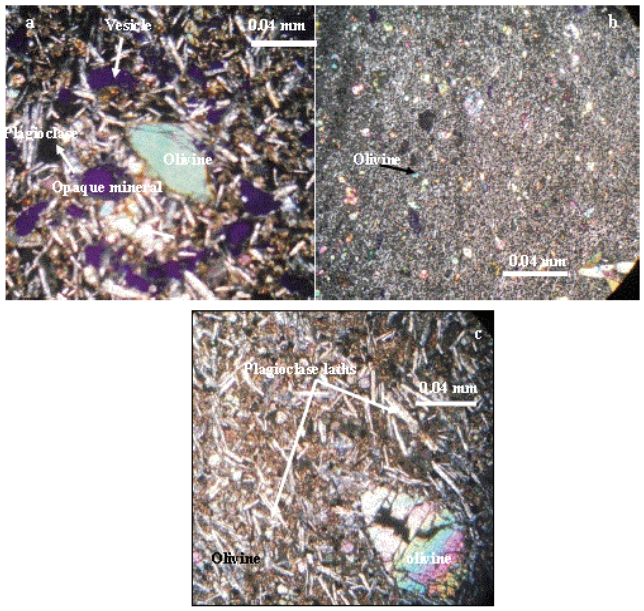

Figure 6: Microphotographs for basanite and picro-basalt (a and b: basanites; c: picro-basalt).

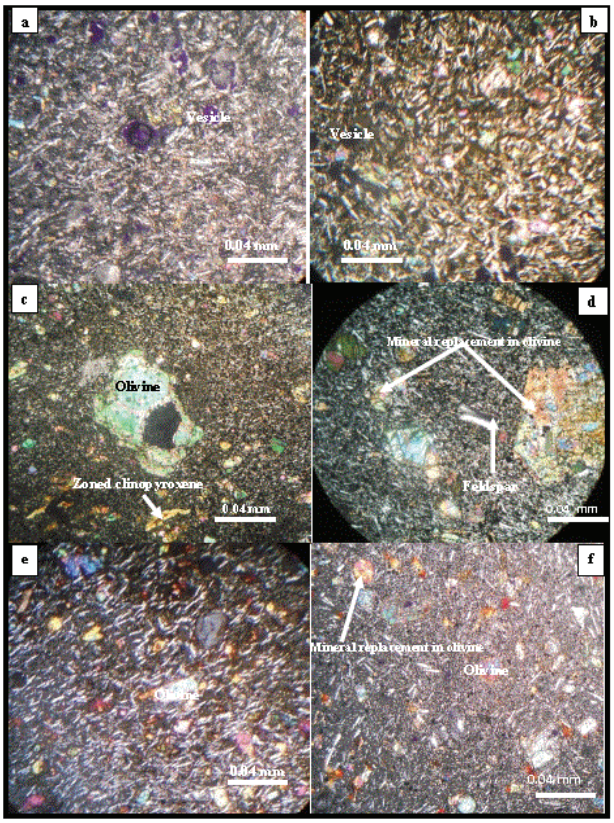

Figure 7: Microphotographs for basalts (a: vesicular-aphanitic rock in Nkogho; b: vesicular- aphyric to microporphyritic rock in Kembong, c: vesicular-aphyric to slightly porphyritic in Talangaye; d: vesicle free-porphyritic rock in Nkogho; e: vesicle free-weakly fluidal and porphyritic rock in Ossing; f: vesicle free-porphyritic rock in Araru).

(Figure 5b). Vesicle diameter ranges from 0.5 mm to more than 1.0 cm (with a depth of up to 2 cm). In Nkogho, basanites are vesicle-depleted (<8% in each collected sample). Vesicle diameter in this rock is up to 5 mm, whereas the depth is below 2 mm. Basanites from Ekok are melanocratic, and aphanitic to slightly porphyritic. Plagioclase laths (Figure 6a) form 65% a very fine-grained groundmass, that includes olivine (17%) and clinopyroxene (8%) phenocrysts (anhedral to euhedral, >0.2 mm) and micro-phenocrysts (sub-hedral to euhedral, >0.01 mm) and opaque mineral (10%) grains (anhedral to subhedral, <0.01 to ≤ 0.03 mm in size). Basanite from Nkogho (Figure 6b) is melanocratic, aphanitic and composed of olivine, plagioclase, clinopyroxene and opaque minerals whose proportion is not easily estimated. Basanite from Babi has a very fine-grained groundmass dominated by plagioclase laths (up to 60%) and has a weakly fluidal structure. Olivine phenocryst (5%) and microphenocrysts (up to 25%), along with microlitic clinopyroxene and opaque minerals (10%) form the remainder of the rock. Picro-basalt is melanocratic when fresh (Figure 5c) and reddish-yellow when partly weathered. Some fragments enclose quartz fragments, and sparse olivine macrocrysts suggest a porphyritic texture (Figure 6c). Plagioclase laths (45%), dominant in the fine-grained groundmass, which hosts euhedral to anhedral fractured olivine (48%) phenocrysts (<1.7 mm) and microphenocrysts (0.03-0.07 mm), clinopyroxene (5%) are mostly sub-hedral microphenocrysts (up to 0.05 mm). Opaque minerals (3%) occur mostly as microlites (≤ 0.01 mm). Basalts are dark-grey, massive and very fine-grained. Some are vesicular while others are not (Figure 5e and 5f). Vesicular fragments are found in a dyke (south of Nkogho) and in patches within southern Kembong and Talangaye. Vesicular basalts from Nkogho are aphanitic (Figure 7a) and contain plagioclase (75%), olivine (10%), clinopyroxene (5%), opaque minerals (10%) and some irregular vesicles. Slightly aphyric to microporphyritic, vesicular fragments from Kembong (Figure 7b) have a similar mineralogy to those from Nkogho, but differ in the size and proportion of plagioclase laths and other materials. Plagioclase laths (70%) dominate in a fine-grained groundmass. Euhedral (four or six sided prisms) and anhedral (mostly sub-rounded) olivine (15%) and pyroxene (10%) microphenocrysts (0.03-0.05 mm) are included within feldspar laths, while spotted vesicles and opaque mineral (sub-hedral to

anhedral, <0.015 mm in size) complete the groundmass. The grain size of minerals differentiates basalts from Talangaye from those at Nkogho and Kembong. Talangaye basalts are aphyric to weakly porphyritic, with partly corroded olivine phenocrysts (5 wt. %; up to 0.3 mm), locally zoned clinopyroxene microphenocrysts (10%, up to 0.06 mm) and opaque minerals (15%) and vesicles disseminated in a very fine-grained groundmass dominated by plagioclase (70%) microlite (Figure 7c). Vesicle-barren basalts from fragments and flows in Nkogho, Ossing, Araru and Babi have similar compositions, but differ in proportions of their minerals. In Nkogho, the basalts are porphyritic (Figure 7d), with olivine (20%) and clinopyroxene (5%) forming anhedral and euhedral (four, six or eight sided prisms) phenocrysts (0.1-0.3 mm), and/or microphenocrysts (0.03-0.08 mm) in a fine-grained plagioclase-rich (65%) groundmass that includes opaque mineral (10%). Some thin sections show microphenocrystic nepheline characterized by grey-white simple twinning. Brownish-red to yellow mineral replacement alters some olivine phenocrysts (Figure 7d), when observed under crossed-polar light. Basalts from Ossing (Figure 7e) are similar to those from Nkogho, but show a weakly fluidal structure, lack common mineral replacement and do not carry nepheline. Dominant plagioclase

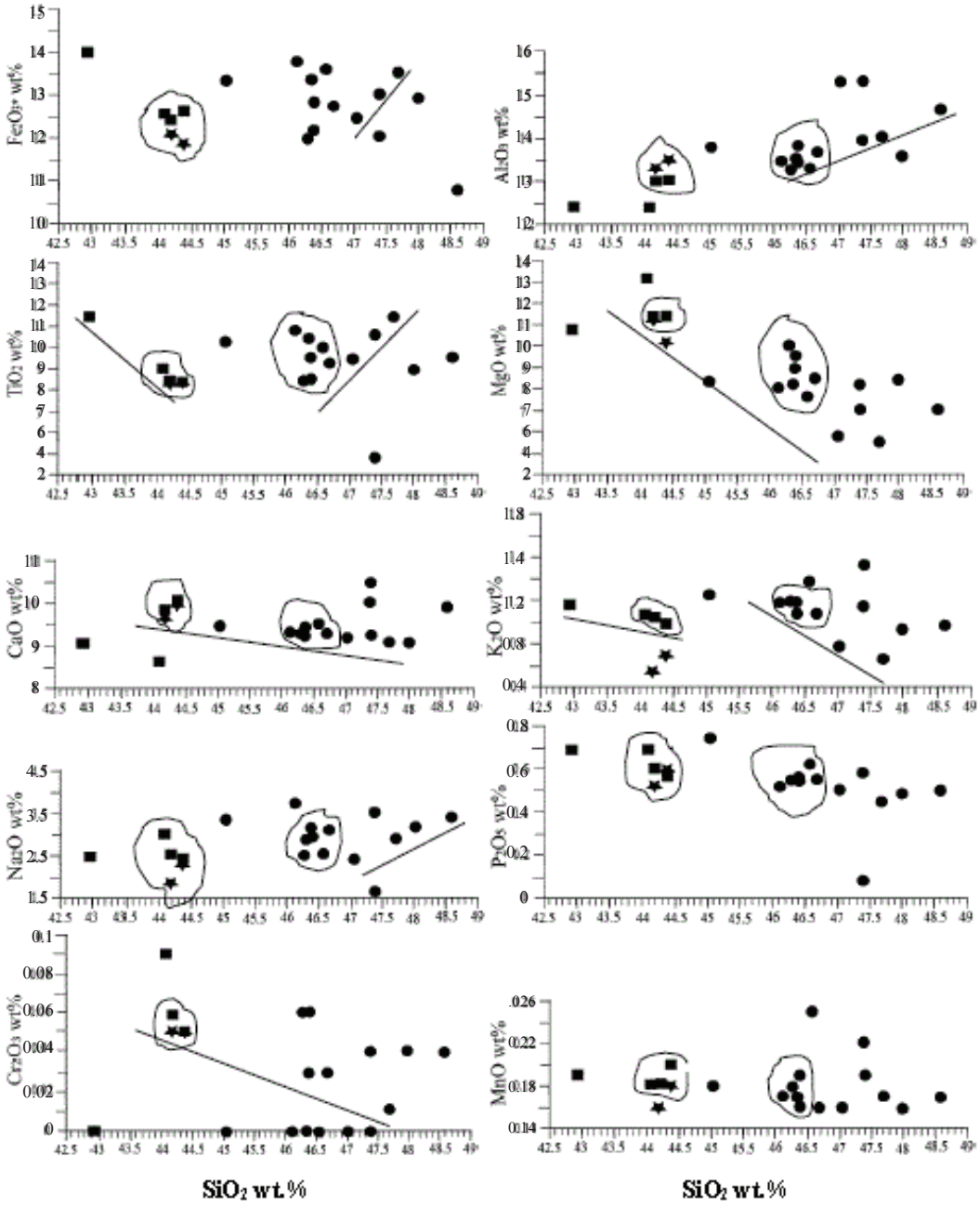

Figure 8: Variation of major and minor element oxides (in wt. %) in the west and southern Mamfe mafic volcanic rocks versus SiO_2. The line the shows either the decrease or increase in major and minor elements contents with that of SiO_2.

(up to 80%) mostly occurs as microlite. Olivine (10%) forms anhedral to euhedral phenocrysts (up to 0.15 mm) and microphenocrysts (below 0.03 mm), clinopyroxene crystals (≤ 8%) are mostly sub-hedral microphenocrysts (≤ 0.03 mm), and opaque mineral (≤ 2%), are set within the feldspathic groundmass. In Babi and Araru (Figure 7f), basalts resemble Nkogho porphyritic basalts, but lack nepheline and fluidal structure. Cracks in olivine locally enclose yellowish products. Proportionally, olivine is estimated at 8%, plagioclase at 72%, clinopyroxene at 10% and opaque mineral at 10%.

Geochemistry

Major and minor element oxide (wt. %) and trace (including rare earth) element (ppm) concentrations in the analyzed rocks are presented in terms of rock types. The calculated CIPW norms are presented with the major and minor element values.

Major and minor element geochemistry: For twenty analyzed samples in Table 1, SiO_2 contents range from 42 to 48 wt. %: in basalts, from 42 to 44 wt. % in basanites; slightly over 44 wt. % in picro-basalts and from 45 to 48 wt. % in basalts. The TiO_2 contents (0.8-3.6 wt. %) show the highest values in basalts. The TiO_2 abundance in basalts distinguishes: low Ti-basalts ($TiO_2 \leq 0.8$ wt. %), mid Ti-basalts ($TiO_2 \leq 2$ wt. %, and high Ti-basalts ($TiO_2 \geq 2$ wt. %) [55,56]. The SiO_2 versus oxide plots in Figure 8 lack major variation; although some plots vary in oxide content with the increase in SiO_2. General grouping of rocks suggest some genetic relationships.

The Al_2O_3 contents range from 12.4 to 13.6 wt. % in basanites, ≤ 13.5 wt. % in picro-basalts and 13.3 to 15.4 wt. % in basalts. Four samples (NKK10, BAI4, ARK16, and KEG2) have elevated alumina contents (>14 wt. %). The Al_2O_3 versus SiO_2 plot (Figure 8) defines both a low-Al group and high-Al group. The calculated Al_2O_3/TiO_2 ratio ranges from 3.95 to 19.90 with the highest ratio for ARK16. The Fe_2O_3 contents range from 11.8 to 14.0 wt. % in basanites, <12.1 wt. % in picro-basalts and from 10.7 to 13.8 wt. % in basalts.

The MgO abundances range from 10.0 to 13.2 wt. % in basanites, ≤ 11.3 wt. % in picro-basalts, and range from 5.4 to 11.0 wt. % in basalt. The basalts show MgO contents from 5.0 to 8.0 wt. % are within the range limit (2.0 to 8.0 wt. %) of Hagos et al. [6] for highly to moderately fractionated mafic rocks. The Mg number values range from 40 to 64, and most values being <55. The highest Mg values were found mainly in picro-basalt and basanite. The plotted oxides versus Mg# in Figure 9 show some decrease of SiO_2, TiO_2, and Fe_2O_3 with Mg# increase, and partly, the increase of Al_2O_3 and K_2O when Mg# increases. The CaO contents range from 9.0 to 10.1 wt. % (basanites), <11.0 wt. % (picro-basalts) and range from 9.1 to 10.5 wt. % in basalts.

The Na_2O contents in wt. %, range from 2.4 to 3.0 in basanite, ≤ 2.9 (picro-basalts) and 1.6 to 3.8 in basalts. The K_2O abundances are: <1.2 wt. % in basanites, ≤ 0.7 wt. % in picro-basalts and 0.6 to 1.6 wt. % in

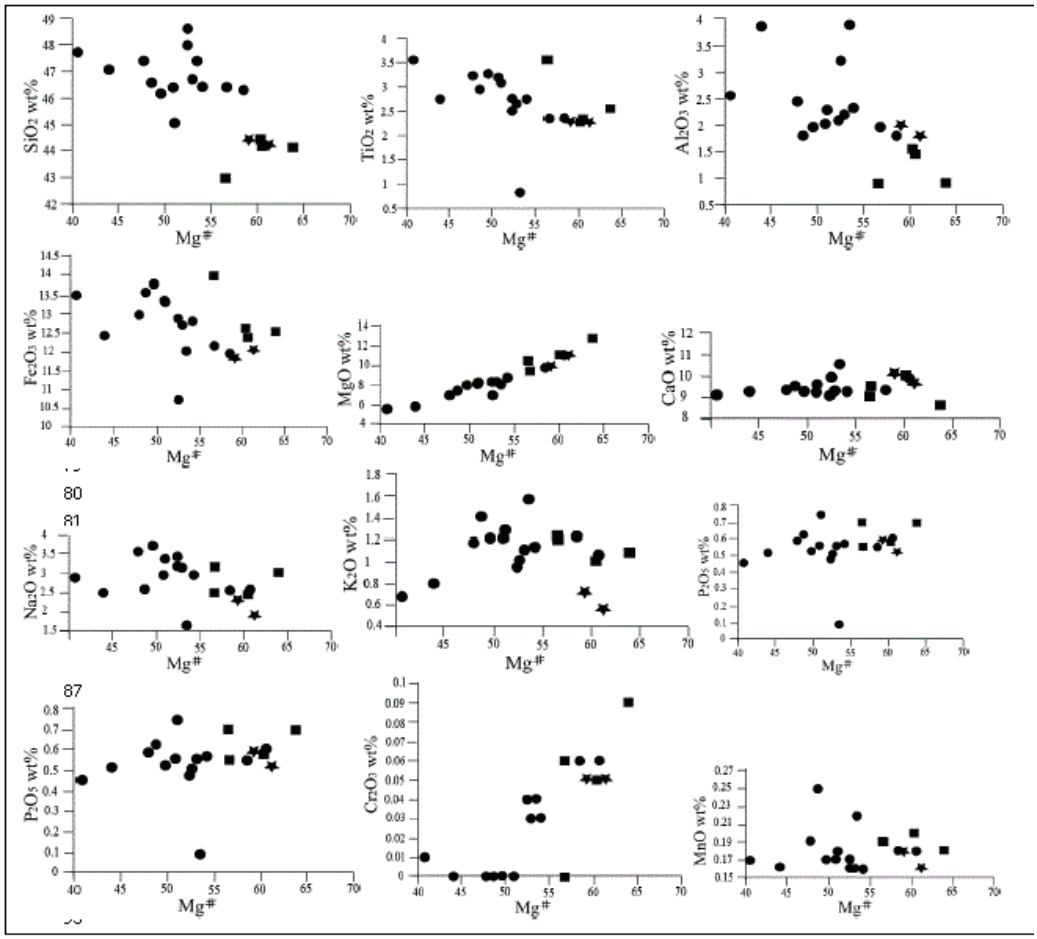

Figure 9: Variation of major element oxides (in wt. %) in the west and southern Mamfe mafic volcanic rocks versus Mg#.

basalts. The Na_2O/K_2O ratios range from 1.0 to 4.4, mostly being less than 2.2 and are lowest in sub-alkaline basalts from Kembong (KEG2), Araru (ARK16) and Babi (BAI4). The alkalinity index $(Na_2O+K_2O)-(0.37*SiO_2-14.43)$ ranges from 0.1 to 2.8 with the lowest values in sub-alkaline picro-basalts and basalts. The sub-alkaline basalts are also termed tholeiitic basalts [2,57,58]. The west and southern Mamfe basaltic rocks mostly belong to the Na-series in a Na_2O versus K_2O binary diagram (Figure 3b) [59]. A few plot within the K-series or on the line separating the two fields.

The MnO contents are mostly between 0.16 to 0.19 wt. %, although EKK1, ARK16 and OSG are higher. The P_2O_5 contents generally range from 0.4 to 0.8 wt. %, except for a low value for ARK16 (0.08 wt. %). Basanites and a Kembong basalt (KEG2), shows high LOI (2.60 to 3.5 wt. %). Low LOI contents (0.46 to 2.02 wt. %) mainly prevail in picro-basalts and basalts.

The CIPW norms in Table 1 show most basanites are nepheline and olivine normative. Picro-basalts, most basalt (e.g., NSI3, NKK1 and NKK7) and a transitional basanite (EKK1) are hypersthene and olivine normative. Some tholeiitic basalts (KEG2, TAE2, OSG and BAI4) are quartz and/or wollastonite normative, other alkali basalts are nepheline and olivine normative (NSI2 and NKK4).

Trace element geochemistry: Trace element abundances for thirteen selected samples in Table 2 and Figure 10 (few elements) show variations related to petrographic rock type. Figure 10a shows groupings of rocks that increase in SiO_2 contents, whereas Figure 10b partly shows variations in trace elements with increase in Mg#. Significant trace element ranges in the rock suites include Ba (≤ 436 ppm: basanites; ≤ 2090 ppm: picro-basalts; and 173-800 ppm: basalts), Cr (342-616 ppm: basanites; 342: picro-basalts; 68-411 ppm: basalts); and Sr (≤ 755 ppm: basanites; ≤ 625 ppm: picro-basalts; 142-722 ppm: basalts). Other important elements are Zr (170-230 ppm: basanites; 170 ppm: picro-basalts; 50-221 ppm: basalts), V (≤ 222 ppm: basanites; ≤ 241 ppm: picro-basalts; 190-239 ppm: basalts), Zn (≤ 120 ppm: basanites; ≤ 141 ppm: picro-basalts; 91-143 ppm: basalts) and Ni (≤ 387 ppm: basanites; ≤ 252 ppm: picro-basalts; 52-193 ppm: basalts). Similar Zr contents (170 ppm) and other trace elements in basanites and picro-basalts from Ekok suggest an affinity between the two rock

Sample composition	Basanites			Picro-basalts		Basalts							
Trace elements (ppm)	BAI3	EKK1	EKK3	EKK6	EKK11	NSI2	NSI3	NKK1	NKK2	NKK6	NKK10	ARK16	BAI4
Ba	385	400	436	2090	519	706	609	358	332	473	797	173.5	218
Zr	230	170	170	170	170	220	210	190	170	160	160	50	190
V	202	214	222	234	241	198	198	201	206	191	199	274	328
Zn	114	118	120	141	124	128	124	134	134	126	140	92	142
Sr	755	726	658	625	588	721	693	597	556	505	561	142.5	411
Rb	21.6	21.4	24	14.7	11.1	28.2	31.2	22.1	23.2	21.3	13.2	76.6	6.8
Ga	19.9	20.2	21.2	21.2	21.8	21	20	22	20.8	21.9	24.1	16.9	24
Y	28.2	22.2	22.8	24.5	24.2	22.7	23.1	23	21.7	21.8	25.5	18.4	32
Nb	53.8	48.5	53.4	46.4	48	50.4	51.3	48	43.9	39.9	38.7	5.3	22.7
Ni	387	237	233	254	252	182	192	156	151	157	156	74	52
Co	49	54	49	66	57	51	54	45	48	46	61	51	44
Cu	56	63	62	64	65	54	54	59	59	54	61	30	57
Sc	18	21	21	22	22	19	18	18	17	18	19	36	26
Pb	5	8	11	15	11	9	8	5	9	7	6	14	4
Ta	3.1	2.7	3.1	2.8	2.7	3.2	2.9	2.8	2.7	2.3	2.7	0.3	1.3
Hf	5.5	4.4	4.5	4.5	4.4	5.6	5.1	4.9	5	3.9	4.5	1.8	5
Th	3.6	4	4.4	4	4.1	4.9	4.7	4.1	3.5	3.1	3.5	1.4	1.9
U	1	1	1.1	1.1	1	1.2	2.2	1	1	0.8	1	0.3	0.5
W	<1	1	1	<1	<1	<1	1	<1	<1	<1	<1	1	<1
Sn	3	1	2	2	2	2	1	2	2	2	2	2	2
Mo	1	2	2	2	2	1	2	1	1	1	2	<1	<1
Cd	<0.5	<0.5	<0.5	<0.5	<0.5	<0.5	<0.5	<0.5	<0.5	<0.5	0.7	<0.5	<0.5
Ag	<0.5	<0.5	<0.5	<0.5	<0.5	<0.5	<0.5	<0.5	<0.5	<0.5	<0.5	<0.5	<0.5
As	<5	<5	<5	5	<5	<5	<5	<5	<5	<5	<5	<5	<5
Cr	615.79	342.11	410.56	342.11	342.11	410.53	410.5	205.26	205.26	273.68	273.68	273.68	68.42
K	8965.6	8301.5	8799.57	5811.04	4482.8	9961.78	10128	9131.6	9048.6	7803.4	8135.46	12867	5562
Ti	15227	13609	13848.4	13668.6	13609	13908.4	13908	16426	15887	14928	16426.3	4796	21222
P	3011	2487.4	2618.3	2574.7	2269.2	2400.09	2400	2443.7	2400.1	2094.6	2181.91	349.11	1964
Rare earth elements (ppm)													
La	42.4	33	36.6	34.7	32.4	38	35.1	30.6	28.8	24.3	27.8	5.8	20.9
Ce	87.1	62.9	71.2	65.2	62.6	71.3	68.9	62.5	58	49.7	54.8	12.9	45.8
Pr	10.6	7.2	8.1	7.5	7.2	8.3	7.7	7.4	7	5.9	6.7	1.4	6
Nd	46.9	32.4	34.7	31.8	32	36.3	34.2	32.8	31.6	27.5	31.3	7.7	28.5
Sm	9.1	6.8	7.2	6.9	6.3	7.2	7	7	6.4	6.2	7.1	2.2	7
Eu	3.2	2.3	2.5	2.4	2.5	2.5	2.4	2.5	2.5	2.2	2.4	0.6	2.6
Gd	8.8	6.6	6.7	6.4	6.3	6.6	6.7	6.9	6.9	6.5	7	2.5	7.5
Tb	1.3	0.9	1	1	0.9	1	1	1	0.9	0.9	1	0.5	1.2
Dy	6	4.4	4.8	4.7	5	5.2	4.9	5.1	4.8	4.5	5.3	2.9	6.1
Ho	1.2	0.9	0.9	1	0.9	0.9	0.9	0.9	0.8	0.9	0.9	0.7	1.2

Er	2.8	2.2	2.4	2.3	2.4	2.4	2.1	2.2	2	2	2.3	2	3.3
Tm	0.4	0.2	0.3	0.3	0.3	0.3	0.3	0.3	0.2	0.3	0.3	0.3	0.4
Yb	2.1	1.7	2	1.6	1.7	1.8	1.6	1.5	1.4	1.5	1.6	2.2	2.5
Lu	0.3	0.2	0.3	0.3	0.3	0.2	0.2	0.2	0.2	0.2	0.3	0.3	0.4
Calculated ratios and anomalies													
Rb/Sr	0.029	0.029	0.036	0.024	0.019	0.039	0.045	0.037	0.042	0.042	0.024	0.538	0.017
Zr /TiO2	90.55	74.89	73.59	74.56	74.89	94.83	90.52	69.34	64.15	64.26	58.39	62.7	53.67
Y /Nb	0.524	0.458	0.427	0.528	0.504	0.45	0.45	0.479	0.494	0.546	0,659	3.49	1.41
Th/U	3.6	4	4	3.64	4.1	4.08	2.14	4.1	3.5	3.875	3.5	4.67	3.8
Zr/Hf	41.82	38.64	37.7	37.7	38.64	39.29	41.18	38.78	34	41.03	35.56	27.77	38
Nb/Ta	17,35	17,96	17,22	16,57	17,77	15,75	17,68	17,14	16,26	17,35	14,33	17,66	17,46
Ba/Nb	7.15	8.25	8.16	45.04	10.81	14.01	11.87	7.46	7.56	11.85	20.59	32.74	9.61
Zr/Nb	4.28	3.51	3.18	3.66	3.54	4.37	4.09	3.96	3.87	4.01	4.14	9.43	8.37
Nb/U	53.8	48.5	48.55	42.18	48	42	23.3	48	43.9	49.88	38.7	17.67	17.46
Th/La	0.085	0.121	0.12	0.115	0.013	0.129	0.134	0.134	0.122	0.128	0.126	0.241	0.091
Ba/La	9.08	12.12	11.91	60.23	16.02	18.58	17.35	11.7	11.53	19.47	28.67	29.91	10.43
Nb/La	1.269	1.47	1.459	1.337	1.481	1.326	1.462	1.569	1.524	1.642	1.392	0.914	1.086
Ce/Pb	17.42	7.86	6.47	4.35	5.9	7.91	8.61	12.5	6.44	7.1	9.13	0.92	11.45
(Ce/Yb)N	11.01	9.82	9.45	10.82	9.78	10.16	11.43	11.06	11	8.8	9.09	1.56	4.86
(La/Yb)N	13.77	13.24	12.48	14.79	13	13.89	14.96	13.91	14.03	11.05	11.85	1.8	5.7
(Tb/Yb)N	2.77	2.37	2.24	2.8	2.37	2.49	2.8	2.98	2.88	2.68	2.8	1.02	2.15
Eu/Eu*	0.74	0.74	0.75	0.77	0.84	0.74	0.74	0.79	0.84	0.81	0.77	0.69	0.88
LREE	140.1	103.1	115.9	107.4	102.2	117.6	111.7	100.5	93.8	79.9	89.3	20.1	72.7
MREE	68	48.1	51.1	47.5	47.1	52.6	50.3	49.2	47.4	42.4	47.8	13	45.6
HREE	14.1	10.5	11.7	11.2	11.5	11.8	11	11.2	10.3	10.3	11.7	8.9	15.1
∑REE	222.2	161.7	178.7	166.1	160.8	182	173	160.9	151.5	132.6	148.8	42	133.4
LREE /HREE	9.94	9.82	9.91	9.59	8.89	9.97	10.15	8.97	9.11	7.76	7.63	2.26	4.82

Table 2: Trace and rare earth element abundance for mafic rocks from the west and southern part of Mamfe Basin (Manyu Division, SW Cameroon) [The Eu/Eu* was calculated following similar method in Kamgang et al. Eu/Eu*=EuN / (SmN × NdN)1/2 with EuN, SmN, NdN being chondrite-normalized values of those elements [34]. Sample location, EKK: Ekok; BAI: Babi; NSI: Nsanaragati; NKK: Nkogho; ARK: Araru; KEG: Kembong; TAE: Talangaye; and OSG: Ossing].

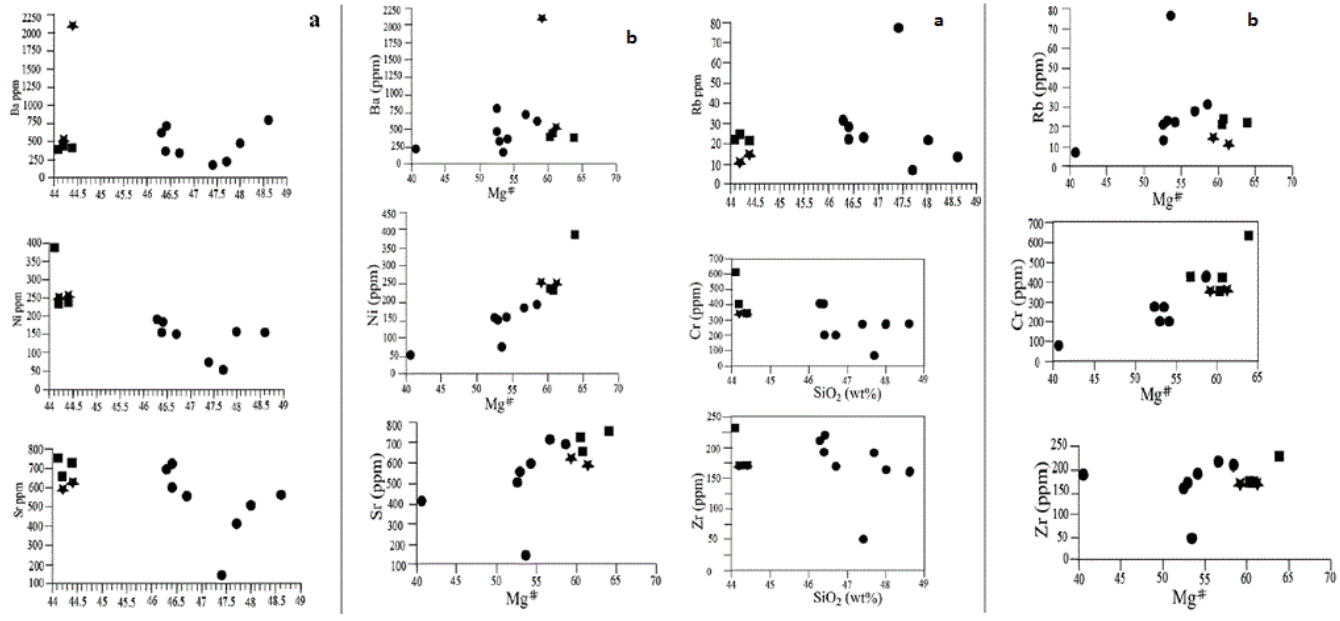

Figure 10: Variation of selected trace element (in ppm) in the west and southern Mamfe volcanic rocks (a: trace element versus SiO_2; b: trace element versus Mg#).

types, as in the trace element versus silicate plot diagrams (Figure 10a). The Zr/TiO_2 ratios vary from 53 to 95 with the lowest values found in NKK10, ARK16 and BAI4. Relatively higher Ni contents are recorded in picro-basalts and basanites, with the lowest values being among the sub-alkaline basalts. The Ni contents in the Mamfe mafic volcanic rocks generally exceed those of many mafic rocks of the Cameroon Volcanic

Line [34,58,60]. The relative high Ni content in the picro-basalts and basalts suggests enrichment of this element in the source magma and its incorporation into olivine.

Rubidium, Ga, Nb, Y, Co, Cu, and Sc abundances are generally low (<70 ppm), with Rb being relatively low in picro-basalts and tholeiitic basalts. Niobium content is lowest in basalt samples (ARK16:5.3 ppm, BAI4:20.7 ppm). The Rb/Sr ratios range from 0.01 to 0.53 with most values being <0.05 (within the limit:<0.07 in mantle peridotite [58]. The Y/Nb and Zr/Nb ratios range from ≤ 0.65 to >1.00 and 3.5 to 10.0, respectively. Lead, Hf, Th, Ta, U, W, Sn, Mo, Cd, Ag, and As contents are very low, ranging from <5 to ≤ 15 ppm. The Zr/Hf, Th/U and Nb/U ratios range from 27 to 42; 2 to 5 and 17 to 50 respectively. The Y/Nb versus Zr/Nb, Zr/Nb versus Zr/Y, and Zr versus Nb diagrams (Figure 11) discriminate between the alkali and transitional tholeiitic basaltic rocks suggesting lower to higher degrees of partial mantle melting were involved in the source magmas.

The primary mantle-normalized trace element patterns (Figure 12a and 12b) show weakly negative Th and strongly negative K anomaly in basanites and picro-basalts [61]. Thorium anomalies are weakly to strongly negative in basalts, whereas the K anomaly is generally weakly negative, except in ARK16 which is strongly positive (Figure 12c). Weakly positive Ba and weakly to strongly positive Pb anomaly feature in the basanites, picro-basalts and alkali basalts.

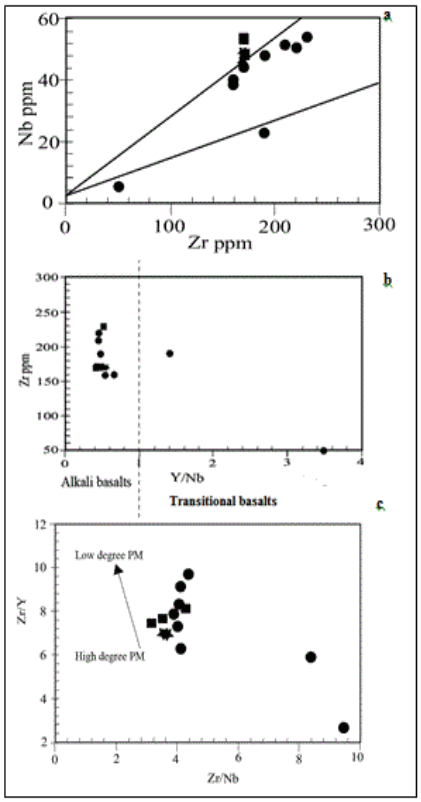

Figure 11: (a) Nb versus Zr plot diagram showing that basanites, picro-basalts and basanites from west and southern Mamfe Basin represent two different magma types. (b) Zr versus Y/Nb plot diagram distinguishing two basaltic groups. The boundary (by dashed) is from Pearce and Cann [64] (c) Zr/Y against Zr/Nb plot showing qualitative trend of compositions resulting from low versus high degrees of partial melting of the west and southern basaltic rocks (PM: primary mantle partial melting).

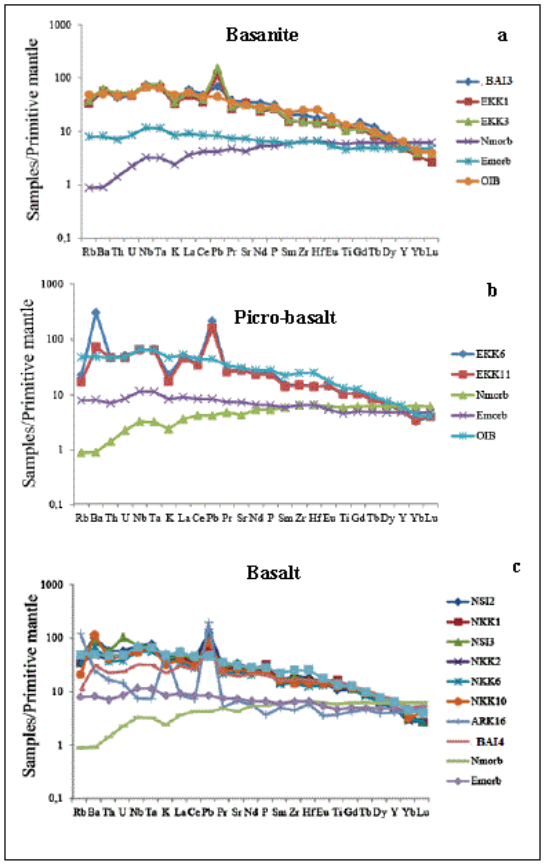

Figure 12: Primitive mantle-normalized multi-element patterns for west and southern Mamfe Basin volcanic rocks. a): basanite, b): picro-basalt, c): basalt. The normalizing values and the values of OIB, N-MORB and E-MORB are from Sun and McDonough [61].

Rare earth element geochemistry: The REE suites for thirteen selected samples (Table 2) show some variation and the domination of light rare earth elements (ΣLREE:20-142 ppm) over middle (ΣMREE:13-68 ppm) and heavy rare earth elements (ΣHREE:8-16 ppm). The total REE ranges from 41 to 223 ppm are generally higher in basanites and picro-basalts. The LREE /HREE ratios range from 2 to 10, with the lowest values in sub-alkaline basalts. Values within the lighter REE in the rock suites include: La (≤ 42.4 ppm:basanites; ≤ 34.7:picro-basalt; 5-39 ppm: basalts), Ce (≤ 87.1 ppm: basanites; ≤ 65.2 ppm: picro-basalt; 12-72 ppm: basalts), Nd (≤ 46.9 ppm: basanites; ≤ 32 ppm: picro-basalt; 7-37 ppm: basalts). The Pr, Sm, Gd, and Dy contents (<11 ppm), are relatively low, while Eu, Ho, Tb, Er, Ho, Tm, Yb and Lu contents (<3.0 ppm) are very low. The calculated Eu anomaly as Eu/Eu* ranges from 0.6 to 10.0 with no marked Eu anomalies on the chondrite normalized REE patterns (Figure 13). The $(La/Yb)_N$ and $(Tb/Yb)_N$ ratios ranges from 1.8 to 15.0 and 1.0 to 3.0, respectively. The highest degree of LREE enrichment $(La/Yb)_N$>10 is predominantly found in basanites, picro-basalts and alkaline basalts. Part of the $(Tb/Yb)_N$ ratios lie within the range (1.89-2.45) for alkali basalts from Hawaii which are considered to have been generated in a garnet-bearing lherzolitic mantle [62].

The chondrite normalized REE patterns (Figure 13) generally show a distinction between basanites in Ekok and those in Babi and between alkaline basalts and some of the tholeiitic basalt (e.g., BAI4). Basanites

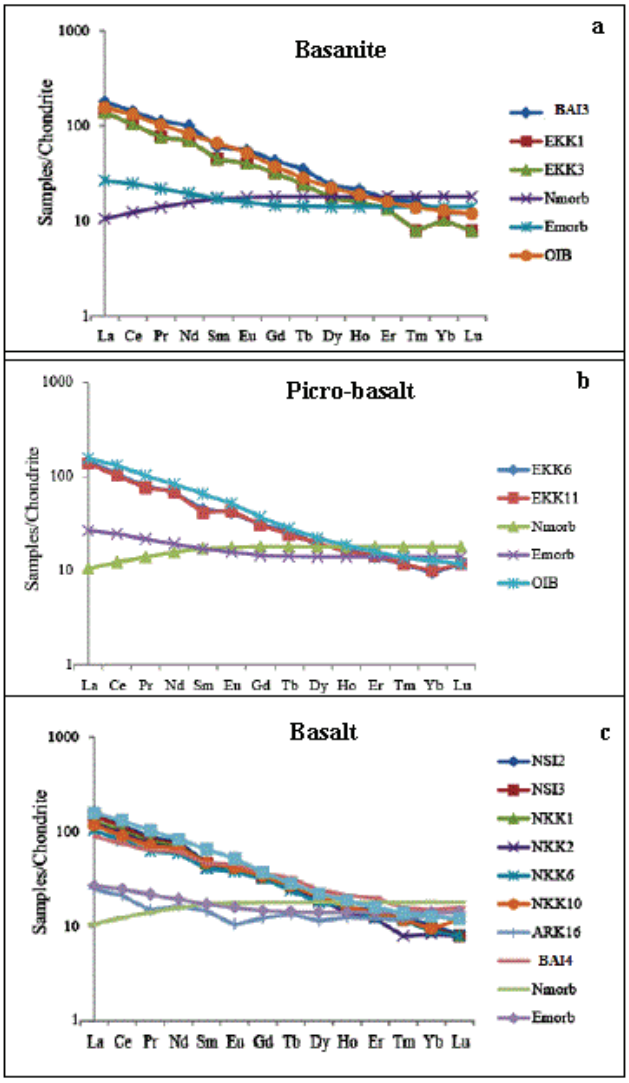

Figure 13: Chondrite normalized rare earth element patterns for west and southern Mamfe Basin volcanic rocks. a): basanite, b): picro-basalt, c): basalt. Values of chondrite and for OIB, N-MORB and E-MORB are from Sun and McDonough [61].

in Ekok show negative Tm and positive Yb anomalies, whereas no Tm and Yb anomalies are shown for basanite from Babi. The Yb anomaly is negative in picro-basalts (Figure 13b) and in some basalt (Figure 13c).

Distinct incompatible trace element characteristics of these rocks include: large variation of total rare earth element (ΣREE) contents (41-223 ppm) and trace and rare earth element ratios such as Nb/La (0.9-1.7) and Ba/Nb (7.1-46.0). Two other key parameters are: Ce/Pb=0.9-17.5 and Th/La=0.01-0.25.

Discussion

The obtained field, petrographic, and geochemical data are discussed separately to characterize each rock type, to help understand the overall petrogenetic history.

Field data and petrography: Basanites form variously vesiculated flows that show blocky to irregular jointing. They resemble pillow lava and lack rubbly base and top (common in 'aa' type flow), and also lack columnar cooling joints. Pillow lavas indicate eruption into water or under ice [2,9]. The basanites probably cooled in water related to the overlying conglomeratic sedimentary deposits. The overlying flow (vesicle depleted in Ekok, Figure 4a and 4b) has a very smooth top, a feature found in pahoehoe flow [2,9,63]. Alternatively, the smoothness of the surface may be due to mechanical action of running water. A feature that supports the pahoehoe nature of this flow is the presence of vesicles in its inner part. The interior of pahoehoe lava is usually vesicular, often containing over 20% vesicles by volume. The pahoehoe nature of the basanite may typify cooling of low-viscosity basaltic lava [2]. The cemented conglomeratic clasts (Figure 4b) at the contact between the lower and upper flows suggest that they are products of two different magmatic eruptions. The hardened clasts are derived from the less consolidated surrounding conglomerates. The elongate parts of the vesicles may indicate either shearing during flow or later flattening, and the high concentration of vesicles towards the top of the lower basanite indicates a lava flow rather than a sill [9]. The aphyric basanites suggests rapid crystallization of melts lacking large suspended crystals and slightly porphyritic basanites a different stage of crystallization: when phenocrysts, grew in a magmatic chamber before rapid cooling at the surface produced a fine grained groundmass [1,2,7,9]. The more porphyritic basanites may signify some crystal fractionation and accumulation, as interpreted by Deshmukh [8].

Picro-basalts form blocky large fragments with some elongation, with visible smooth and prismatic surface features common in columnar flows [9]. Although picro-basalts can form in flows and dykes, it is difficult ascertain their exact origin in the Mamfe Basin. Topographically, these rocks are found at the hilly part in Ekok (at about 200 m), showing that the source was probably a volcano. This geomorphology (high topography) may suggest the presence of a local magma chamber under this hilly area. Geophysical survey is needed to confirm the existence of this magmatic chamber, as its crystallization history is not easily interpreted by simple observation of fragments at the surface. The vesicles represent gas bubbles that form when molten lava becomes supersaturated with volatiles on ascent and their absence in the picro-basalts suggests an origin from volatile-depleted magma. Xenocrystic quartz with thin contact metamorphism zones suggest it came from post sedimentary materials from the surrounding sandstones. Olivine and clinopyroxene macrocrysts and microcrysts, in a very fine-grained ground mass in the picro-basalts may suggest three stages of crystallization: macrocrysts (slow cooling in a magmatic chamber); microcrysts (shallow depth cooling) and groundmass (rapid cooling at the surface) [8].

In summary, basalts occur as volcanoclasts in SW Nkogho and Nsanaragati, as eluvial fragments in Talangaye and Babi, pillow-like lava in Kembong, Araru and Ossing, and as a dyke in south Nkogho. Volcanoclasts probably come from nearby volcanoes as most occur at the foot of hills (mainly in Nkogho). The presence of pillow lava suggests aqueous involvement and a basaltic dyke intruding granitic basement in Nkogho provides age control for the tectonic fracturing and volcanic events. Sedimentary rocks in the Mamfe Basin were affected fracturing and volcanic events as they were over-run by lava and are locally cut by unstudied mafic dykes. Vesicle-rich basalts (e.g., Nkogho dyke, Kembong flow) and vesicle-poor basalts (e.g., Talangaye and Babi fragments, Araru and Ossing flows) mark two groups of magmas of different volatile contents. Textural difference in aphyric or porphyritic basalts suggests different cooling histories in magma production. Modal nepheline in basalt from Nkogho typifies an alkaline and undersaturated nature [2,7]. Pseudomorphous mineral replacement of olivine (Nkogho basalt) by secondary mineral products

such as serpentine and iddingsite suggests low-grade metamorphism or hydrothermal alteration of basalts by exposure to hot circulating fluids [2].

Geochemical features and classification: The major elements and CIPW norms data in Table 1 differentiate the basanites, picro-basalts and basalts. Among the basanites (ultrabasic with SiO_2<45 wt. %) the Nkogho basanite has the lowest SiO_2 (<43 wt. %) and highest Fe_2O_3 (<13 wt. %) and the Babi basanite shows the highest MgO (<13 wt. %) and Mg# (~64) [1]. The basanites are nepheline-olivine normative rocks, but one transitional type (EKK1) is hypersthene-olivine normative. The picro-basalts are ultrabasic, but hypersthene-olivine normative [2]. The picro-basalts differ in the total alkali versus silica diagram of Irvine and Baragar, as one (EKK6) plots slightly in the alkaline field and another (EKK11) in the sub-alkaline field [54]. They show highest LOI values (2.9 to 3.5 wt. %), which may affect their precise chemical designations. In most of the Harker plots diagrams (Figures 8 and 9) the alkaline picro-basalt (EKK6) plots close to transitional basanite from Ekok. They may be products of allied magmas, as they have similar plots in many discriminating diagrams (Figures 10, 11b, 11c and 14). The basalts differ from the other rocks in higher SiO_2 (>45 wt. %, basic: Al_2O_3 (>13 wt. %), Na_2O (dominantly>2.90 wt. %) and lower MgO (≤ 10 wt. %) and Mg# (40-59) [1]. Some of those major element contents are within the ranges of basanite found in Mount Bamenda, Cameroon volcanic line basalts although the basanites there are consistently higher in Na_2O contents [34]. In the Irvine and Baragar binary diagram three groups of Mamfe basalts are distinguished: (1) alkaline basalts; (2) sub-alkaline basalts; and (3) those plotted on the alkaline-subalkaline dividing line [54]. The transitional nature of some is confirmed by Y/Nb versus Zr plots (Figure 11a) [64]. The CIPW norms distinguish four groups: (1) nepheline-olivine bearing basalts (NSI1 and NKK4); (2) olivine-hypersthene bearing basalts (e.g., NSI3, NKK1, NKK2, and ARK16); (3) hypersthene-quartz basalts (TAE and BAI4); and (4) quartz-wollastonite bearing basalts (KEG2 and OSG). Based on Gill, three groups of basalts can be separated on presence or absence of normative quartz or nepheline: (1) silica oversaturated basalts (with quartz and no nepheline); (2) silica-saturated (no quartz or nepheline); and silica undersaturated (with nepheline) [2]. By combining the plots in Irvine and Baragar diagrams with the CIPW norms, nepheline-olivine rocks and part of olivine-hypersthene basalts are alkaline, whereas the wollastonite-quartz-bearing basalts are all sub-alkaline (tholeiitic) [54]. Basalts that plot on the divide line separating the sub-alkaline and alkaline fields are hypersthene-olivine normative. Altogether, it is then possible to distinguish seven groups of Mamfe Basin basalts: alkaline nepheline olivine basalts; alkaline olivine-hypersthene basalts; alkaline hypersthene-quartz basalts; transitional hypersthene-olivine basalts; wollastonite-quartz tholeiitic basalts; and hypersthene-olivine tholeiitic basalts. The Al_2O_3 (>13 wt. %) content in tholeiitic basalts is greater than the values (10.88 and 12.49 wt. %) in Rajahmundry (India) tholeiitic basalts. The Al_2O_3 difference between the Mamfe tholeiitic basalts and those of Rajahmundry shows that cooling magma never had the same chemical enrichment, as most of the other elemental contents are not the same.

The Mamfe Basin mafic volcanic rocks mainly plot in the Ocean Island Basalt field using a FeOt, MgO and Al_2O_3 ternary diagram (Figure 14) [65]. A few plot within the continental field or on the line separating the Mid-Ocean Ridge and Ocean Island Basalt fields. These plots suggest that the studied rocks mainly formed from three different sources of magma. Some match geochemical features of Indian Ocean basalts described in Hagos et al. and differ to mafic volcanic rocks in Mount Bamenda [6,34]. The basalts erupted at mid-ocean ridges are olivine tholeiitic basalts characterized by high silica content (up to 50 wt. %) and very low K_2O content [2]. The geochemical features in tholeiitic basaltic rocks in this study differ to those of continental tholeiitic rocks presented in Ngounouno et al [57]. The Sr abundances in Mamfe basaltic rocks are similar to those of basaltic rocks in Mount Bamboutos (≤ 1963 ppm: which are low strontium basaltic rocks (LSrB) [66]. The extreme variation of Ba contents (173 to 2090 ppm) lead to distinction of two groups of Mamfe basaltic rocks: high Ba basaltic rocks (HBaBr) and low Ba basaltic rocks (LBaBr). The only HBaBr is a picro-basaltic sample (EKK6).

Petrogenetic and tectonic evaluation: Basalt magmas produced by melting in the Earth's mantle range in their geochemistry, and carry up a variety of deep inclusions. So their study can elucidate the nature of the underlying upper mantle and even aspects of the composition of the lower mantle [2]. Petrogenetic interpretation of basaltic suites rocks can be approached by evaluating the behavior of less mobile elements (e.g., Ti and Al) and certain key trace elements (Nb, Cr, Co, Zr, Y and some REE). In the nearby Cameroon volcanic line, basaltic studies analyzed Mg# values and the Ni and MgO contents [58,60]. The Mg# values in primitive upper mantle lavas range from 68 to 72 and are also characterized by high Ni (300-500 ppm), Cr (300-500 ppm) and Co (50-70 ppm) contents [67,68]. The Mg# values (40-64) for the studied Mamfe volcanic rocks are too low for the primitive limit defined by Green and O'Hara [67]. BAI3 is the sample closest to primary features with relatively high Mg# (64), Ni (387 ppm), Cr (616 ppm) and Co (49 ppm). Within the mafic rocks, the Mg# values (40-44) for part of quartz-wollastonite and quartz-hypersthene basalts are more evolved than the other mafic rocks (Mg#: 47-64). For the Mg# values for less evolved rocks (46.3-66.1), also fall short of primitive mantle basalts. A more evolved source for some of those rocks are supported by their low MgO (<9 wt. %) and Ni (<75 ppm). The source magmas for those more evolved rocks could be generated from fractionation processes in mantle-derived magmas [60]. The alkaline nature of the Mamfe mafic rocks is reflected in their enrichment in incompatible elements and high fractionation indexes, $(La/Yb)_N$ ranging from 11-15. These values lie within the range (10.62-22.80) in alkaline mafic volcanic rocks studied by Kamgang et al. [34]. The high $(La/Yb)_N$ indicating relative enrichment of LREE and depletion in HREE was considered

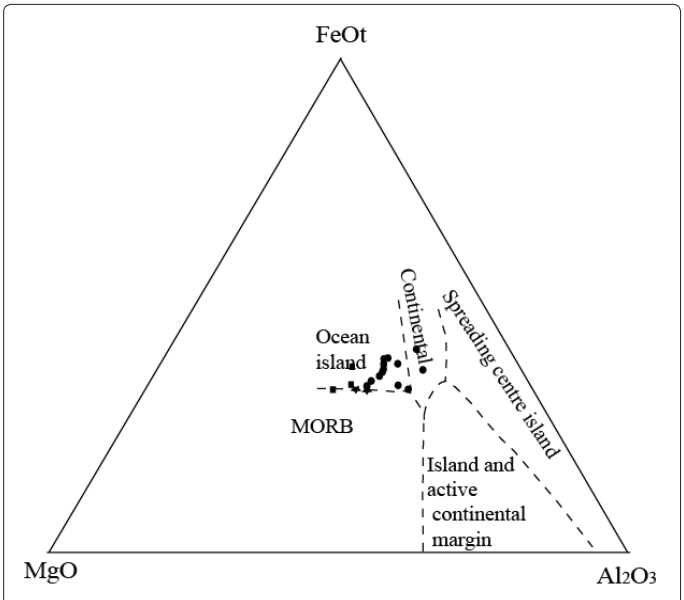

Figure 14: Plots for west and southern Mamfe mafic volcanic rocks in Pearce et al. [65] FeOt, MgO and Al_2O_3 ternary plot diagram.

to denote residual garnet in the source for these magmas and would likely apply also to the alkaline rocks from the Mamfe Basin. The other similarity is their $(Tb/Yb)_N$ >2.0, which are high and within the range limit for Bamenda Mountain mafic rocks 1.8-3.0 [34]. For Wang et al. high $(Tb/Yb)_N$ in mafic volcanic rock also characterizes the presence of residual garnet in the mantle source [69]. The calculated residual garnet proportions for the Mamfe rocks are shown in Figure 15. The high Ba contents mainly in Mamfe basanites and picro-basalts may stem from phlogopite in their magma sources based on the Zhao et al. and Ngounouno et al. studies [57,70].

The LILE, Nb, Zr, and Y contents in Ekok picro-basalt (EKK6) and basanites are similar. EKK6 may be a product from fractional crystallization in the magma source for the basanites. This is supported by the grouping and variation within plots in Figures 8-12. Figures 8-10, show grouping between Ekok basanites and EKK6. In a diagram (Figure 14), EKK6 and EKK3 (basanite) plot in Ocean Island Basalt and Mid Ocean Ridge Basalt fields. In general, crystal fractionation forms part of the processes that formed the range of mafic rocks within the Mamfe Basin. This reflected in the Harker diagrams, including trends in Ni and Cr contents and moderate Mg# values (≤ 64).

The geochemical behavior of the High Field Strengths Elements (HFE) such as Nb, Ta, Zr and Hf makes it possible to explore the mantle sources by using Zr/Hf and Nb/Ta ratios which are less changeable during crustal contamination and crystal differentiation processes [71,72]. Ratios of Nb/Ta (17-18: basanites; 16-18: picro-basalts; 14-18: basalts) and Zr/Hf (37-42: basanites; up to 38.4: picro-basalts; 27-42: basalts) for Mamfe mafic rocks in some case match those of primitive mantle (17.5 ± 2.0) and 36.27, respectively. This suggests the magmas for part of the basaltic rocks were derived from mantle sources without obvious crustal contamination. The ratios of La/Ce, Sm/Nd, Ce/Nb, Zr/Nb, of the basaltic rocks, however, differ from primitive mantle values (Table 4), being enriched in LREE and reflecting fertilized mantle sources [70]. Basalt ARK16 is depleted in Nb, Ti, Zr, Ta and Hf and enriched in Rb and has significant Sm, Ce, and Ba contents. This feature is similar to some mantle enclaves in south Hunan Province, China, where it was suggested to fingerprint mantle metasomatism [70]. The magma of this sample probably formed in a mantle containing metasomatic reactions. The Cr and Ni contents in Mamfe basanites, picro-basalts and part of alkaline basalts are higher than those of the tholeiitic basalts (e.g., ARK16). This suggests that the degree of partial mantle melting may be lower in the Cr-Ni relative enriched rocks and higher in the tholeiitic basalts [70]. The highly incompatible element ratios such as Zr/Nb, K/Nb, Ba/Th, Th/La, Ba/La and Ba/Nb (Table 4) are shown to be least susceptible to fractionation during partial melting, and are not significantly fractionated during limited degrees of low-pressure crystallization of OIB magmas [73]. Hence they could be useful indicators for basaltic end-member characterization of the Mamfe basaltic rocks. As presented in Figure 16 and Table 4, the mantle source magmas for alkaline, transitional and tholeiitic basaltic rocks from the Mamfe Basin are mainly influenced by the EM1 end-member in term of Nb/Th and Zr/Nb ratios, and by the HIMU-EM1 end-member in term of Zr/Y and Nb/Y ratios.

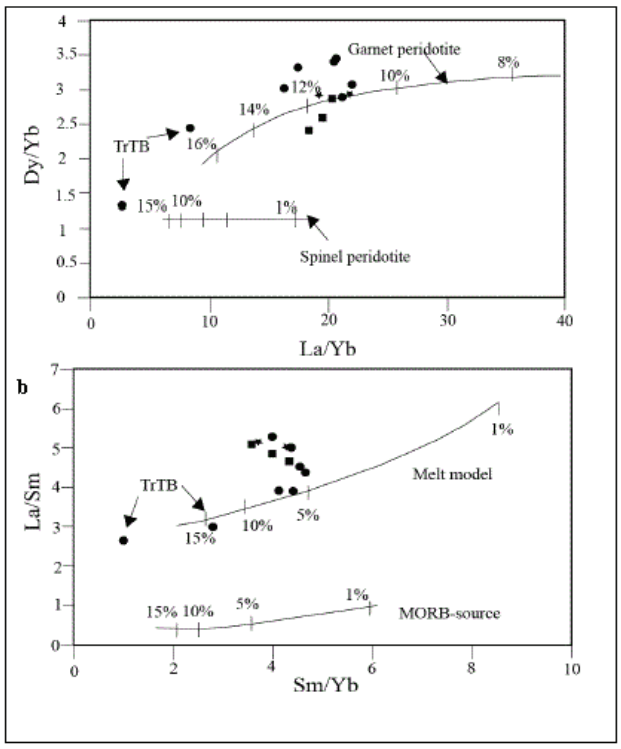

Figure 15: Plots for west and southern Mamfe volcanic rocks in two source discriminating diagrams. (a) La/Yb *vs.* Dy/Yb plot trend lines show degrees of partial mantle melting for garnet peridotite and spinel peridotite [78,79]. (b) Sm/Yb *vs.* La/Sm plot gives the melt plot trend lines are inverse batch partial mantle melting model and the depleted MORB source composition. TrTB (Transitional Tholeiitic Basalt) lie apart from the other plots and near higher degrees of melting generated from enriched source composition relative to N-MORB from Sun and McDonough [61].

Basaltic volcanic rocks are erupted in a wide variety of tectonic environments (e.g., mid-ocean ridges, island arcs, back-arc basins, intra-plate oceanic islands, large igneous provinces and intra-continental rifts) [2]. Basaltic rocks in the western Mamfe Basin plot within the Ocean Island Basalt (OIB) and transitional fields (plots on the line separating OIB and Mid Ocean Ridge Basalt MORB) fields, whereas, the southern rocks are mainly OIB type and a few continental basalts. These OIB types can be distinguished by relative high contents of incompatible trace elements (e.g., Nb, Zr, Ta, Ba, Sr) and the relative low content of these elements in the continental basalts. The latter are probably post-rifting and post-Cretaceous volcanic products, formed after the likely Cretaceous opening of the W-E branch of the Benue Trough (Mamfe Basin). They are dominantly post-sedimentation as they locally overlie or cross-cut the sedimentary rocks in this basin.

Potential uses of the mafic rocks: Rocks such as the Mamfe basalts, picro-basalts, and basanites are mined and used as industrial mineral in civil engineering for construction of road and houses [20,21]. Some can host interesting concentration of elements (e.g., significant Al abundance: native and Mills; sulfide metallic deposits, or placer gemstones derived from xenocrysts or xenoliths [13,14,16,17,31,32,74]. Except for one significant concentration of Ba (2090 ppm in EKK6) and one elevated Ni value (387 ppm) most elements in the studied exposures are not sufficiently concentrated. No gemstone deposits or gem-host xenoliths were found. The above rocks, however, may have potential for some sources of industrial materials as building and road-constructing materials, or possibly aluminous sources in weathered form. The parent rock of lateritic bauxite deposits at Fongo-Tongo and Bangam in the western Cameroon is an aluminum-enriched basalt (Al_2O_3: up to 15.6 wt. %: Table 3) [74]. These Al-enriched basalts are always of interest for lateritic bauxite prospecting as they can produce accumulation of Al in soil profiles during intense weathering and

Sample number and/or locality	Si2O	Ti2O	Al203	Fe2O3	MnO	MgO	CaO	Na2O	K2O	P2O5	Cr2O3	LOI
Fongo-Tongo	43.4	3.9	15.5	11.64	-	8.47	9.78	3.15	1.72	1.O9	-	-
Bangam	47.2	4.53	15,6	13,75	-	4.35	8.3	3.9	1.82	-	-	0.61
Araru (ARK16)	47.4	0.8	15.35	12	0.2	8.2	10.5	1.66	1.55	0.08	0.04	2.02
Kembong (KEG2)	47.05	2.73	15.35	12.43	0.16	5.79	9.19	2.49	0.78	0.51	-	3,07

Table 3: Comparing major element geochemical composition (in wt. %) for Al-enriched basalts from West Cameroon Fongo-Tongo and Bangam and south of the Mamfe Basin (Araru and Kembong).

Ratio	La/Ce	Sm/Nd	Ce/ N d	Zr/Nb	La/Nb	Ba/ N b	Ba/Th	Rb/Nb	K/Nb	Th/Nb	Th/La	Ba/La
PM(7)	0.384	0.325	1.35	14.8	0.94	9	77	0.91	323	0.117	0.125	9.6
Crust(7)				16.2	2.2	54	124	4.7	1341	0.44	0.204	25
EMI(7)				5.3-11.5	0.86-1.19	11.4-17.8	103-154	0.88-1.17	213-432	0.105-0.122	0.107-0.128	13.2-16.9
EMII(7)				4.5-7.3	0.89-1.09	7.3-11.0	67-84	0.59-0.85	248-378	0.111-0.157	0.122-0.163	8.3-11.3
Study rocks												
Basanites	0.487-0.525	0.194-0.210	1.85-2.06	3.1-4.3	0.68-0.79	7.1-8.3	100-110	0.40-0.50	164-172	0.066-0.083	0.085-0.121	9.0-12.2
Picro-basalts	0.518-0.532	0.197 -0.217	2.05-2.23	3.1-3.7	0.68-075	10.8-45.1	130-523	0.23-0.32	93-125	0.086	0.013-0.115	16.0-60.3
Basalts	0.456-0.535	0.198-0.306	1.60-2.02	3.5-9.5	0,61-1,09	7.4-32.8	87-228	0.30-14.45	190-2428	0.072-0.264	0.091-0.241	10.4-30.0

Table 4: Trace element characteristics of different mantle end-members and basaltic rocks from the west and southern part of Mamfe Basin (Manyu Division, SW Cameroon).

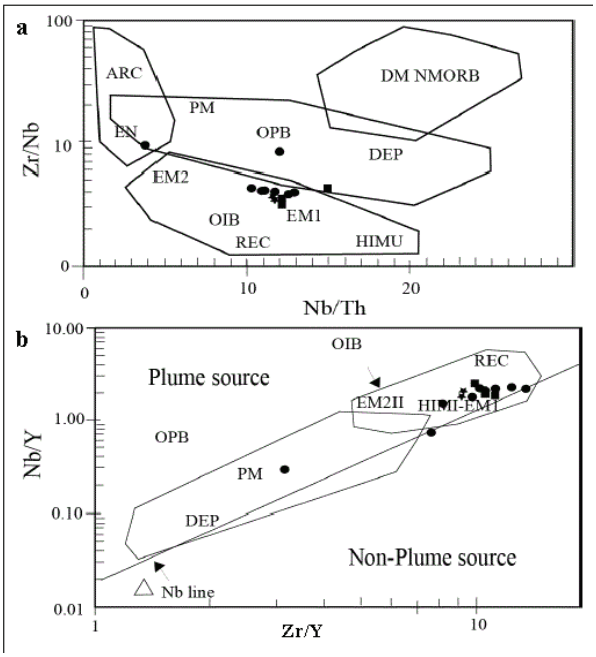

Figure 16: Plots for west and southern basaltic rocks relative to the mantle compositional components (filled star) and fields for basalts from various tectonic settings as defined by Weaver [73] and Condie [80]. (a) Nb/Th–Zr/Nb and (b) Zr/Y-Nb/Y (PM: primitive mantle; DM: shallow depleted mantle; HIMU: high mu (U/Pb) source; EM1 and EM2: enriched mantle sources; ARC: arc related basalts; N-MORB: normal ocean ridge basalt; OIB: oceanic island basalt; DEP: deep depleted mantle; EN: enriched component; REC: recycled component; OPB: oceanic plateau basalt.

element leaching within tropical climate and plateau topography. The Al_2O_3 content (15.35 wt. %) in ARK16 and KEG2 is very close to values found in Fongo-Tongo and Bangam Al-enriched basalts, but are less than values 17.98-20.81 wt. %: for high-alumina basalt in Sant'Antioco Island, SW Sardinia, Italy [75]. ARK16 and KEG2 through chemical weathering within tropical climatic conditions and plateau topography may pay future geochemical prospecting of Al concentration within lateritic soil overlying those basalts for potential bauxite developments.

Diamond occurrences were noted in western Mamfe Sedimentary Basin [26]. Geochemical analyses on coarse-grained detrital zircons show some zircon crystals had kimberlitic affinities [22,27,29,30]. The studied picro-basalts (ultra-basic and mantle origin) are exclusively found on high land (up to 200 m of height) in western Mamfe Basin [2]. The presence of these rocks shows a possible cooling of a mantle ultrabasic rock in this locality. Although not directly an indicator for kimberlite, these mantle source rocks may carry diamond as xenocrysts or in kimberlitic xenoliths showing the existence of kimberlite at shallow depth [2]. Detailed geochemical and geophysical prospecting for kimberlitic or other diamantiferous host rock indicators may lead to discovery of such rocks in that hilly topography.

Conclusions

The west and southern Mamfe mafic volcanic exposures are alkaline, transitional and sub-alkaline rocks including basanites, picro-basalts, and basalts mainly formed during post-sedimentary and tectono-volcanic events. Basanites are dominantly OIB-like undersaturated rocks formed from less evolved mantle source magma. These rocks host the highest nickel concentration. Picro-basalts are alkaline to subalkaline saturated rocks also formed from less evolved mantle source magma. They can host significant concentration of Ba and Ni. Some of these rocks are a product of fractionation of the alkali basalt and basanite source magmas.

Basalts are alkaline and transitional undersaturated rocks, or subalkaline, saturated and oversaturated, rocks formed from variably evolved mantle source magmas mostly representing Ocean Island type sources and include some continental rift basalt types. Some basalt has higher Al contents and has potential for developing bauxite during intense chemical weathering.

Acknowledgements

Special thanks for the two anonymous reviewers whose comments helped to improve this manuscript. We extend our gratitude to Professor Chen Shouyu (China University of Geosciences, Wuhan), who funded part of the major geochemical analysis.

References

1. Le Maitre RW, Streckeisen A, Zanettin B, Le Bas MJ, Bonin B, et al. (2002) Igneous rocks: A classification and glossary of terms. (2nd edn), Cambridge University Press p: 252.
2. Gill R (2010) Igneous rocks and processes: A practical guide. Wiley Blakwell, A John Wiley and Sons Ltd Publication p: 366.

3. Beaux FJ, Fogelgesang FJ, Agard P, Boutin V (2011) Atlas de Géologie Pétrologie. Dunod Paris, p:144.
4. Tchuimegnie NNB, Kamgang P, Chazot G, Agranie A, Bellon H, et al. (2015) Age, geochemical characteristics and petrogenesis of Cenozoic intraplate alkaline volcanic rocks in the Bafang region, West Cameroon. J African Earth Sci 102: 218-232.
5. Le Bas MJ, Le Maitre RW, Streckeisen A, Zanettin B (1986) A chemical classification of volcanic rocks based on the total alkali-silica diagram. J Petrol 27: 745-750.
6. Hagos M, Koeberl C, Kabeto K, Koller F (2010) Geochemical characteristics of the alkaline basalts and the phonolite-trachyte plugs of the Axum area, northern Ethiopia. Aus J Earth Sci 103: 153-170.
7. Winter DJ (2010) Principles of igneous and metamorphic petrology. (2nd edn) Pearson new international production p: 745.
8. Deshmukh SS (1988) Petrographic variations in compound flows of Deccan Trap and their signifance. Memoir Geological Society of India 10: 305-319.
9. Coe LA (2010) Geological field techniques. Wiley Backwell p: 337.
10. Shukla PN, Bhandari N, Das A, Shukla AD, Ray JS (2001) High iridium concentration of alkaline rocks of Deccan and implications to K/T boundary. J Earth Syst Sci 110: 103-110.
11. Crocket J, Paul D, Lala TJ (2013) Platinum-group elements in the Eastern Deccan volcanic province and a comparison with platinum metals of the western Deccan. J Earth Syst Sci 122: 1035-1044.
12. Seifert W, Rhede D, Tietz O (2008) Typology, chemistry and origin of zircon from alkali basalts of SE Saxony (Germany). N Jb Miner Abh 184: 299-313.
13. Sutherland FL, Coenraads RR, Abduryim A, Meffre S, Hoskin PWO, et al. (2015) Corundum (sapphire) and zircon relationships, lava plains gem fields, NE Australia: Integrated mineralogy, geochemistry, age determination, genesis and geographical typing. Mineral Mag 79: 545-581.
14. Watanabe M, Hoshino K, Shiokawa R, Takaoka Y, Fukumoto H, et al. (2006) Metallic mineralization associated with pillow basalts in the Yaeyama Central Graben, Southern Okinawa Trough, Japan. JAMSTEC Report of Res Develop 3: 1-8.
15. Medenbach O, ElGoresy A (1982) Ulvöspinel in native iron-bearing assemblages and the origin of these assemblages in basalts from Ovifak, Greenland, and Bühl, Federal Republic of Germany. Contribution to Mineral Petrol 80: 358-366.
16. Taylor LA, Day JMD, Goodrich CA, Howarth GH, Pernet-Fisher JF, et al. (2014) Metallic-Fe deposits in basalts: Siberia, Greenland, and Germany. International Mineralogical Association, Johannesburg, South Africa.
17. Mills S (2015) Mineralogy and petrology of unique native-iron basalts from northern Siberia. J Undergraduate Res at the University of Tennessee 6: 181-195.
18. Kuepouo G, Sato H, Tchouankoue PJ, Murata M (2008) FeO*-Al_2O_3 -TiO_2 rich rocks of the Tertiary Bana igneous complex, West Cameroon. Resour Geol 59: 69-86.
19. Sababa E, Ndjigui DP, Ebah Abeng AS, Bilong P (2015) Geochemistry of peridotite xenoliths from the Kumba and Nyos areas (southern part of the Cameroon Volcanic Line): Implications for Au-PGE exploration. J Geochem Explor 152: 75-90.
20. Gomes LR, Rodrigues EJ (2006) Physical characterization and weathering of the basaltic rocks of the Paraná Basin, Brazil. IAEG 559: 1-9.
21. Danciu C, Buia G (2009) Classification and characterization of basalts of Branisca and Donra-Romania, for capitalization. Recent Adv Industries and Manufacturing Technologies pp: 64-69.
22. Kanouo SN (2014) Geology of the Western Mamfe Corundum Deposits, SW Region Cameroon: Petrography, geochemistry, geochronology, genesis, and origin. Univ de Yaounde I p: 225.
23. Wilson D (1928) Notes on the geology of the Mamfe Division, Cameroon SW province. Occasional papers. Geologic Survey of Nigeria nº 6.
24. Dumort JC (1968) Geological map of recognition of Cameroon at scale 1/500000 sheet Douala-West, with explanatory note. National Printers, Yaounde Cameroon p: 69.
25. Kanouo SN (2008) Geological study of the sapphire mineralization indexes in the southern part of the Mamfe Sedimentary Basin. Univ de Yaoundé I p: 91.
26. Laplaine L, Soba D (1967) Report of the geological service for the years 1965-1966-1967, prospecting of sapphires in the Cretaceous basin of Mamfe.
27. Kanouo SN, Zaw K, Yongue FR, Sutherland LF, Meffre S, et al. (2012a) U-Pb zircon age constraining the source and provenance of gem-bearing late Cenozoic detrital deposit, Mamfe Basin, SW Cameroon. Resour Geol J 62: 316-324.
28. Kanouo SN, Zaw K, Yongue FR, Sutherland FL, Meffre S, et al. (2012b) Detrital mineral morphology and geochemistry: methods to characterize and constrain the origin of the Nsanaragati blue sapphires, south-western region of Cameroon. J Afr Earth Sci 70: 18-23.
29. Kanouo SN, Yongue FR, Ekomane E, Njonfang E, Ma C, et al. (2015) U-Pb ages for zircon grains from Nsanaragati Alluvial Gem Placers: its correlation to the source rocks. Resour Geol J 65: 103-121.
30. Kanouo SN, Ekomane E, Yongue FR, Njonfang E, Zaw K, et al. (2016) Trace elements in corundum, chrysoberyl, and zircon: Application to mineral exploration and provenance study of the western Mamfe gem clastic deposits (SW Cameroon, Central Africa). J Afr Earth Sci 113: 35-50.
31. Sutherland FL, Schwarz D, Jobbins EA, Coenraads RR, Webb G (1998) Distinctive gem corundum from discrete basalt fields: a comparative study of Barrington, Australia, and west Pailin, Cambodia, gem fields. J Gemol 26: 65-85.
32. Sutherland FL, Graham IT, Pogson RE, Schwarz D, Webb GB, et al. (2002) The Tumbarumba basaltic gem field, New South Wales: In relation to sapphire-ruby deposits of eastern Australia. Records Aus Museum 54: 215-248.
33. Fitton JG (1980) The Benue trough and the Cameroon line a migrating rift system in West Africa. Earth Planet Sci Letters 51: 132-138.
34. Kamgang P, Chazot G, Njonfang E, Ngongang TBN, Tchoua MF (2013) Mantle sources and magma evolution beneath the Cameroon volcanic line: Geochemistry of mafic rocks from the Bamenda Mountains (NW Cameroon). Gondwana Res 24: 727-741.
35. Suchel JB (1972) The distribution of rainfall and rainfall patterns in Cameroon, Talence.
36. Olivry JC (1986) Rivers and Rivers of Cameroon, Paris. Hydrographic Monograph, Orstom p: 734.
37. Ajonina HN, Ajibola OA, Bassey EC (2001) The Mamfé basin, SE Nigeria and SW Cameroon: A review of the Basin filling model and tectonic evolution. J Geosci Society Cameroon 1: 24-25.
38. Bassey CE, Ajonina HN (1997) Petrology of the upper member (Cenomanian) of the Mamfe formation, Mamfe embayment, Southwestern Cameroon. 15th Annual International Conference p: 40.
39. Eyong TJ (2003) Lithostratigraphy of the Mamfe cretaceous basin. South West Province of Cameroon-West Africa p: 256.
40. Eseme E, Littke R, Agyingi MC (2006) Geochemical characterization of a cretaceous black shale from the Mamfe basin, Cameroon. Petrol Geosci 12: 69-74.
41. Njoh OA, Nforsi MB, Datcheu JN (2015) Aptian-late cenomanian fluvio-lacustrine lithofacies and palynomorphs from Mamfe basin, Southwest Cameroon, West Africa. Int J Geosci 6: 795-811.
42. Njoh OA, Njie SM (2016) Hydrocarbon source rock potential of the lacustrine black shale unit, Mamfe basin, Cameroon, West Africa. Earth Sci Res 6: 217-230.
43. Le Fur Y (1965) Special report on corundum research. Archives Office of Geological and Mineral Research p: 69.
44. Eseme E, Agyingi MC, Foba-Tendo J (2002) Geochemistry and genesis of brine emanations from Cretaceous strata of the Mamfe basin, Cameroon. J Afr Earth Sci 35: 467-476.
45. Eyong TJ, Wignall P, Fantong YW, Best J, Hell VJ (2013) Paragenetic sequences of carbonate and sulphide minerals of the Mamfe basin (Cameroon): Indicators of palaeofluids, palaeo-oxygene levels and diagenetic zones. J Afr Earth Sci 86: 25-44.
46. Njonfang E, Moreau C (1996) The mineralogy and geochemistry of a subvolcanic alkaline complex from the Cameroon line, the Nda Ali massif, South-West Cameroon. J Afr Earth Sci 22: 113-132.
47. Kangkolo R (2002) Aeromagnetic study of the Mamfe basalts of Southwestern Cameroon. J Cameroon Acad Sci 2: 173-180.
48. Regnoult JM (1986) Cameroon Geological Synthesis, Ministry of Mines, Sodexic Yaoundé p: 119.

49. Mackenzie SW, Donaldson HC, Guilford C (1982) Atlas of igneous rocks and their texture. British Library Catalogue in Publication Data p: 154.

50. Mackenzie SW, Adams EA (1994) A colour atlas of rocks and minerals in thin section. Manson publishing Ltd p: 98.

51. Mackenzie SW, Guilford C (1998) Atlas for rock-forming minerals in thin section. British Library Catalogue in Publication Data p: 106.

52. Higgins DM (2006) Quantitative and textural measurement in igneous and metamorphic petrology. Cambridge University press p: 273.

53. Wu WY, Li C, Xu JM, Xiong QS, Fan GZ, et al. (2016) Petrology and geochemistry of metabasalts from the Taoxinghu ophiolite, central Qiangtang, northern Tibet: Evidence for a continental back-arc basin system. Aust J Earth Sci 109.

54. Irvine TN, Baragar WRA (1971) A guide to the chemical classification of the common rocks. Canadian J Earth Sci 8: 523-548.

55. Simonov VA, Mikolaichuk AV, Safonova IYU, Kotlyarov AV, Kovyazin SV (2014) Late Paleozoic-Cenozoic intra-plate continental basaltic magmatism of the Tienshan-Junggar region in the SW Central Asian Orogenic Belt. Gondwana Res 27: 1646-1666.

56. Manikyamba C, Ganguly S, Santosh M, Saha A, Lakshminarayana G (2015) Geochemistry and petrogenesis of Rajahmundry trap basalts of Krishna-Godavari Basin, India. Geosci Frontiers 6: 437-451.

57. Ngounouno I, Déruelle B, Guiraud R, Vicat PJ (2001) Tholeiitic and alkaline magmatism of the Cretaceous half-grabens of Mayo Oulo-Léré and Babouri-Figuil (northern Cameroon-South of Chad) in the domain of continental extension. Académie Sci 333: 201-207.

58. Kuepouo G, Tchouankoue PJ, Nagao T, Sato H (2006) Transitional tholeiitic basalts in the tertiary Bana volcano-plutonic complex, Cameroon Line. J Afr Earth Sci 45: 318-332.

59. Middlemost EAK (1975) The basalt clan. Earth Sci Review 11: 337-364.

60. Nkouandou OF, Ngounouno I, Déruelle B, Ohnenstetter D, Montigny R, et al. (2008) Petrology of the Mio-Pliocene volcanism to the North and East of Ngaoundéré (Adamawa, Cameroon). CR Géosci 340: 28-37.

61. Sun S, McDonough W (1989) Chemical and isotopic systematics of oceanic basalts: Implications for mantle composition and processes. Geological Society of London Special Publications 42: 313-345.

62. Frey FA, Garcia MO, Wise WS, Kennedy A, Gurriet P, et al. (1991) The evolution of Mauna Kea volcano, Hawaii: Petrogenesis of tholeiitic and alkalic basalts. J Geophys Res 96: 14347-14375.

63. Allaby M (2008) Dictionary of earth sciences. (3rd edn) Oxford University Press p: 663.

64. Pearce JA, Cann JR (1973) Tectonic setting of basic volcanic rocks determined using trace element analysis. Earth Planet Sci Lett 19: 290-300.

65. Pearce TH, Gorman BE, Birkett TC (1977) The relationship between major element geochemistry and tectonic environment of basic and intermediate volcanic rocks. Earth Planet Sci Lett 36: 121-132.

66. Marzoli A, Piccirillo ME, Renne RP, Bellieni G, Iacumin M, et al. (2000) The Cameroon volcanic line revisited: Petrogenesis of continental basaltic magmas from lithospheric and asthenospheric mantle sources. J Petrol 41: 87-109.

67. Green DH, O'Hara MJ (1971) Compositions of basaltic magmas as indicators of conditions of origin: Application to oceanic volcanism. Philosophica Transactions of the Royal Society of London 268: 707-725.

68. Jung S, Masberg P (1998) Major and trace element systematics and isotope geochemistry of Cenozoic mafic volcanic from the Vogelsberg (Central Germany): Constraints on the origin of continental alkaline and tholeiitic basalts and their mantle sources. J Volcanol Geotherm Res 86: 151-177.

69. Wang K, Plank T, Walker JD, Smith EI (2002) A mantle melting profile across the Basin and range, SW USA. J Geophy Res 107.

70. Zhao Z, Bao Z, Zhang B (1998) Geochemistry of the Mesozoic basaltic rocks in southern Hunan Province. Science in China 41: 103-112.

71. Pfander JA, Münker C, Stracke A, Mezger K (2007) Nb/Ta and Zr/Hf in ocean island basalts: Implications for crust-mantle differentiation and the fate of niobium. Earth Planet Sci Lett 254: 158-172.

72. Huang H, Niu Y, Zhao Z, Hei H, Zhu D (2011) On the enigma of Nb-Ta and Zr-Hf fractionation: A critical review. J Earth Sci 22: 52-66.

73. Weaver BL (1991) The origin of ocean island basalt end-member compositions: Trace element and isotopic constraints. Earth Planet Sci Letters 104: 381-397.

74. Hiéronymus B (1973) Mineralogical and geochemical study of bauxite formations in Western Cameroon. Cahier Orstom Série Géologie 5: 97-112.

75. Conte MA, Palladino MD, Perinelli C, Argenti E (2010) Petrogenesis of the high-alumina basalt-andesite suite from Sant'Antioco Island, SW Sardinia, Italy. Per Mineral 79: 27-55.

76. Benkhelil J (1989) The origin and evolution of the cretaceous Benue trough (Nigeria). J Afr Earth Sci 8: 251-282.

77. Maluski H, Coulon C, Popoff M, Baudin P (1995) $^{40}Ar/^{39}Ar$ chronology, petrology and geodynamic setting of Mesozoic to early Cenozoic magmatisim from the Benue Trough, Nigeria. J Geologic Society of London 152: 311-326.

78. Thirlwall FM, Upton BGJ, Jenkins C (1994) Interaction between continental lithosphere and Iceland plume-Sr-Nd-Pb isotope geochemistry of tertiary basalts, NE Greenland. J Petrol 35: 839-879.

79. Bogaard PJF, Worner G (2003) Petrogenesis of basanitic to tholeiitic volcanic rocks from the Miocene Vogelsberg, Central Germany. J Petrol 44: 569-602.

80. Condie KC (2005) High field strength element ratios in Archean basalts: A window to evolving sources of mantle plume. Lithos 79: 491-504.